Article

Dairying, diseases and the evolution of lactase persistence in Europe

In European and many African, Middle Eastern and southern Asian populations, lactase persistence (LP) is the most strongly selected monogenic trait to have evolved over the past 10,000 years[1]. Although the selection of LP and the consumption of prehistoric milk must be linked, considerable uncertainty remains concerning their spatiotemporal configuration and specific interactions[2,3]. Here we provide detailed distributions of milk exploitation across Europe over the past 9,000 years using around 7,000 pottery fat residues from more than 550 archaeological sites. European milk use was widespread from the Neolithic period onwards but varied spatially and temporally in intensity. Notably, LP selection varying with levels of prehistoric milk exploitation is no better at explaining LP allele frequency trajectories than uniform selection since the Neolithic period. In the UK Biobank[4,5] cohort of 500,000 contemporary Europeans, LP genotype was only weakly associated with milk consumption and did not show consistent associations with improved fitness or health indicators. This suggests that other reasons for the beneficial effects of LP should be considered for its rapid frequency increase. We propose that lactase non-persistent individuals consumed milk when it became available but, under conditions of famine and/or increased pathogen exposure, this was disadvantageous, driving LP selection in prehistoric Europe. Comparison of model likelihoods indicates that population fluctuations, settlement density and wild animal exploitation—proxies for these drivers—provide better explanations of LP selection than the extent of milk exploitation. These findings offer new perspectives on prehistoric milk exploitation and LP evolution.

When our ancestors started to consume the milk of domesticated ruminant animals, they set in motion a sequence of events leading to the evolution of lactase persistence (LP)[6] and ultimately the modern global dairy industry, using about 1.5 billion cattle[7] as the principal milk source. Evidence for prehistoric milk exploitation based on combined faunal and organic residue analysis indicates considerable spatial variability. Analysis of sheep or goat age-at-death profiles suggest that dairy management was concurrent with the domestication of caprines in southwest Asia in the ninth millennium BC[8,9]. The earliest organic residue-based evidence of dairying locates to seventh millennium BC northwest Anatolia and is associated with high proportions of cattle bones in faunal assemblages[2]. It is clear that dairy husbandry and processing technologies were brought by the first farmers into Europe via the Mediterranean coast[3] and through the Balkans[10,11] into central Europe[12–14], although milk use remains undetected in Neolithic sites of northern Greece[15]. In northern Europe, extensive studies of organic residues in pottery and dental calculus show unequivocally that the fourth millennium BC Neolithic inhabitants of the British Isles and Ireland were accomplished dairy farmers (for example, refs. [16–19]). In prehistoric Denmark, there is evidence of milk use alongside aquatic resource processing from 4000 BC (ref. [20]). In prehistoric Finland, the region of highest milk consumption globally today[7], milk use appears with the arrival of Corded Ware pottery in the early third millennium BC, although climate fluctuations may subsequently have triggered returns to hunter–gatherer–fisher subsistence strategies[21,22].

Ancient DNA (aDNA) data indicate that most, if not all, Early Neolithic people were lactase non-persistent (LNP) and that LP only reached appreciable frequencies in the Bronze and Iron Ages[23–28]. Such an allele frequency trajectory indicates strong selection favouring LP and is consistent with selection starting in the Early Neolithic period[28,29]. The main Eurasian LP-causing allele (rs4988235-A, also known as 13,910*T; ref. [30]) has a highly structured geographical distribution in modern Europe[31]. This may reflect different strengths of selection in different regions[32,33], although other explanations also remain plausible, such as modern frequencies being shaped by demographic processes[29,34]—including a suggested Bronze Age Steppe origin[25] (but see ref. [28])—or allele distribution reflecting its origin location[29,35]. A range of suggestions to explain positive LP selection have been proposed[6,24,36–40]. Among these, the calcium assimilation hypothesis[32]—in which milk supplements low vitamin D diets in regions with reduced ultraviolet B radiation, such as occur in northern Europe—is probably the most widely cited[41,42]. However, this hypothesis does not explain the inferred high selection strengths in lower latitude regions, such as Africa, the Middle East, southern Europe and southern Asia[40], where milk as a source of relatively pathogen-free fluid provides a more plausible explanation[36]. Others[33] recently noted a latitudinal cline in the proportion of milk fats in pots in Early Neolithic Atlantic Europe and argued that, as a marker of milk usage, this cline explains the modern LP distribution in the same region. Regardless of the proximal and probably regionally specific drivers of selection on LP, milk consumption
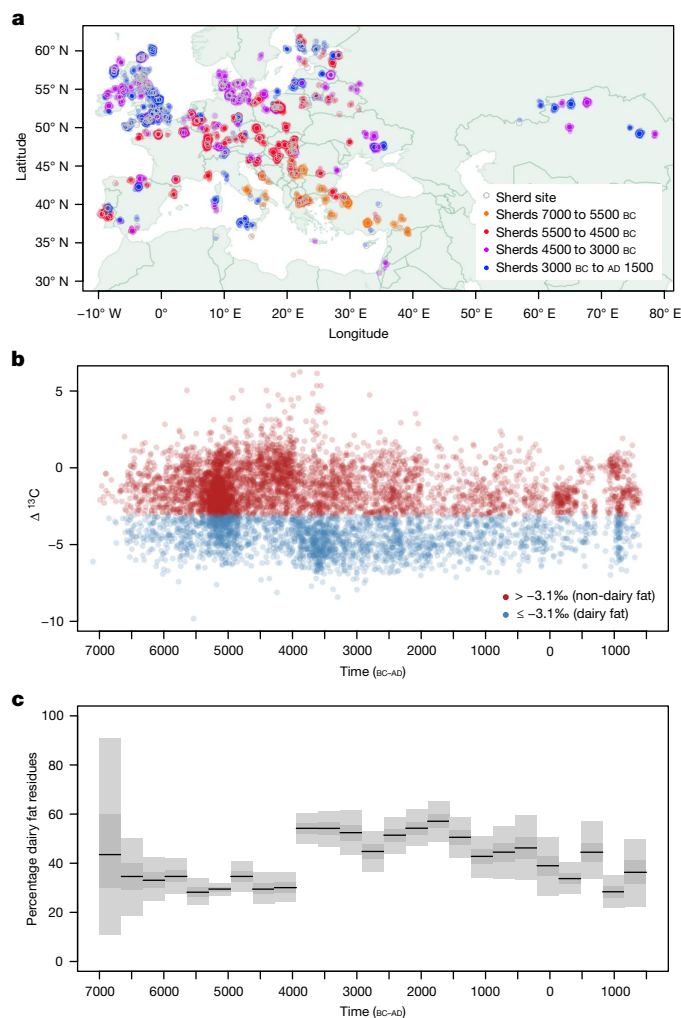
Fig. 1 | Geographical and temporal distribution of archaeological milk fat residues in potsherds. a, Coloured circles illustrate 6,899 potsherds with animal fats from 826 phases from 554 sites (grey circles). Coloured circles are jittered to prevent perfect overlay, enabling the number of sherds to be visualized. **b**, Plot of $\Delta^{13}C$ values for all 6,899 animal fat residues extracted from prehistoric potsherds through time. Each point corresponds to an individual measurement on a potsherd, with its position on the *x* axis randomly sampled from the uniform date range of the associated archaeological phase. Animal fats with $\Delta^{13}C$ values ≤−3.1‰ are defined as ruminant milk fats. Mare's milk is not characterized using this proxy[84] and would thus be defined as 'non-milk'. **c**, Percentage of dairy fat residues through time, calculated using all animal fat residues. Grey bars and black lines illustrate 95%, 50% confidence interval (CI) and maximum a posteriori (MAP) in each time slice, using a uniform prior.

is a prerequisite[43]. However, LP is not accompanied at an individual level by meaningful differences in milk consumption[31,37,44,45] or the risks from a range of diseases[46] in modern populations and thus its selection may be underpinned by potential adverse consequences of milk consumption in LNP individuals only in certain historically contingent environments[37].

Mapping ancient milk use

To build a more comprehensive picture of prehistoric milk use and examine how well it explains selection on LP, we compiled all published instances of the occurrence of milk fat residues detected in pottery containers from 366 archaeological sites in Europe and southwest Asia. To improve spatiotemporal coverage we added newly

generated organic residues data from 188 sites from various regions and periods. Overall, we used 6,899 animal fat residues derived from 13,181 potsherds from 826 phases from 554 sites, with associated georeferences and phase chronology including more than 1,000 radiocarbon dates. These data were used to generate time series depicting the frequency of milk use across prehistoric continental Europe from 7000 BC to AD 1500 (Fig. 1) and regional time series (Fig. 2 and Extended Data Fig. 1). The high density of organic residues around 5500 to 5000 BC in Fig. 1b reflects our new sampling, targeted to explore the coevolution of dairying and LP amongst the first farmers in the central European Linearbandkeramik culture[29]. If we consider the profusion of $\Delta^{13}C$ values ≤−3.1‰ (a proxy for milk fat residues[16,47,48]; Methods; Fig. 1b), it becomes immediately clear that milk use was a very widespread activity across all periods in European prehistory and at the broadest scale this was congruous with the spread of farming across the continent.

The extensive sampling and analysis of pottery has enabled us to resolve the spatiotemporal patterning of milk use in unprecedented detail (Fig. 2). Importantly, this shows that milk exploitation arrived with the first farmers into the Mediterranean basin (except the region covered by modern day Greece) and continued throughout the Neolithic period, whilst the later arrival of the Neolithic in Southern Britain was associated with immediate and high milk use−probably reflecting the arrival of advanced dairying populations from adjacent regions of continental Europe[27]−which then gradually reduced. The prehistoric Balkans was the core region for the early intensification of milk use, which is consistent with the rise of cattle exploitation there[49] yet, surprisingly, milk use appears largely absent from geographically adjacent Neolithic site phases located in Greece (on the basis of analyses of >190 animal fats from >870 potsherds; however, we note that other types of containers may have been used for milk processing in this cultural context). In some regions our data suggest continuous intensive milk use, notably in western France, northern Europe and the British Isles from 5500 BC to AD 1500. Despite intensive sampling from central Europe (>2,800 animal fats from >6,810 potsherds), a region previously inferred to be the origin of selection on LP[29], the frequency of milk use was consistently lower than for the southeast, west or north of Europe throughout prehistory. The overarching picture is that, whilst dairying persisted throughout the Neolithic period, its intensity fluctuated substantially in space and through time, suggesting regionally specific instabilities in food production and cultural changes in dietary preferences. This is consistent with previous studies showing regional 'boom and bust' fluctuations in population density across Europe over the same period[50].

Milk use and LP evolution

LP allele (rs4988235-A) frequency trajectory estimates (Fig. 3) based on published aDNA data from 1,786 prehistoric European and Asian individuals ('Data' under 'Ancient DNA analyses' in Methods), are well-described by a sigmoidal curve, as expected for a selective sweep. Curves fitted only to aDNA broadly predict modern allele frequencies[31]. We note that, although the allele only reaches appreciable frequencies by about 2000 BC (ref. 28), nearly three millennia after its first detection (earliest LP individual dated to about 4700–4600 BC), the dates of origin, the start of selection, the earliest observation and the reaching of appreciable frequencies of this allele are all distinct 'events', each possibly separated by thousands of years[28]. To examine if milk usage patterns can explain these allele frequency trajectories, we devised a maximum likelihood modelling approach (Methods), whereby LP selection intensity was determined by the proportion of potsherds with dairy fat residues (as a proxy for milk use). Using simulations, we made sure that our approach had the power to detect an association, if there was one, even in the presence of moderate levels of noise in our milk use patterns ('Power analysis' under 'Ancient DNA analyses'
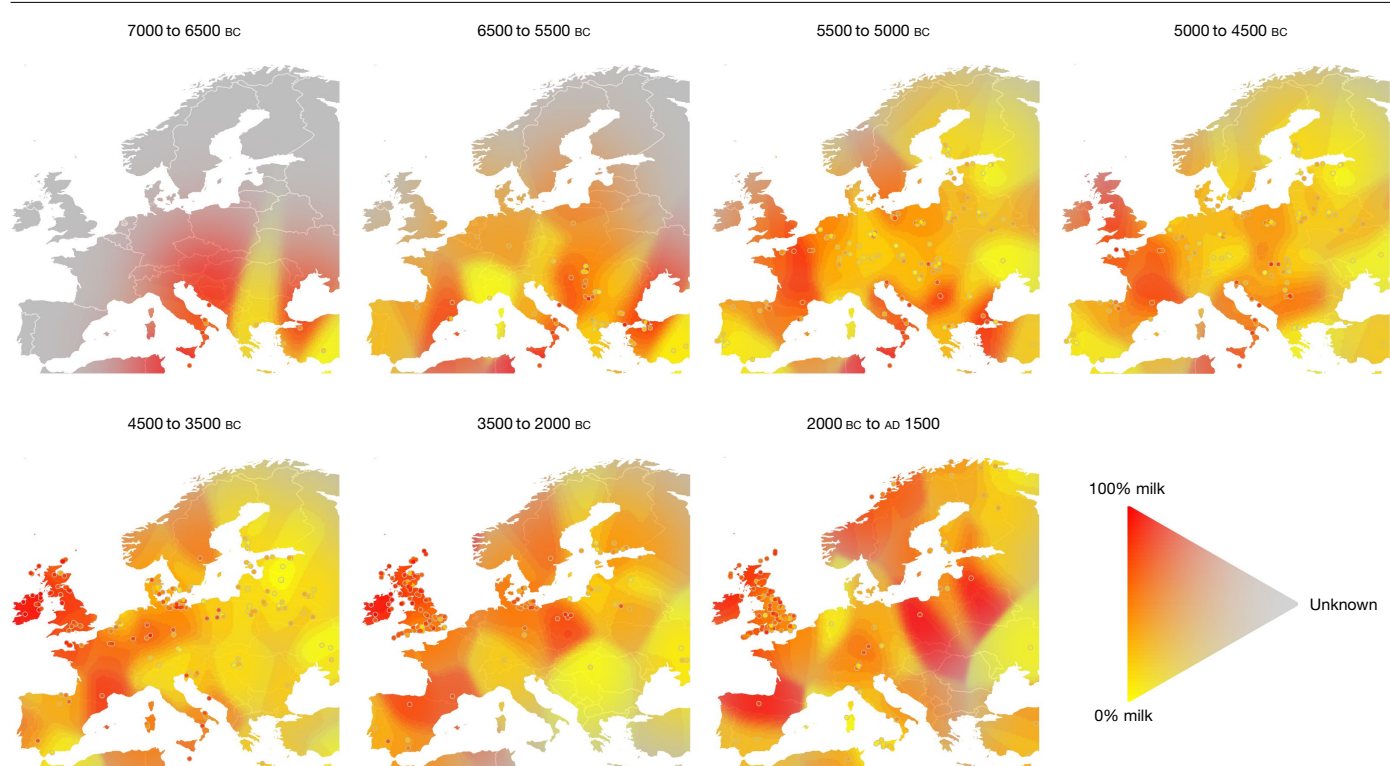
Fig. 2 | Regional variation in milk use in prehistoric Europe. Interpolated time slices of the frequency of dairy fat residues in potsherds (colour hue) and confidence in the estimate (colour saturation) using two-dimensional kernel density estimation. Bandwidth and saturation parameters were optimized using cross-validation. Circles indicate the observed frequencies at site-phase locations. The broad southeast to northeast cline of colour saturation at the beginning of the Neolithic period illustrates a sampling bias towards earliest evidence of milk use. Substantial heterogeneity in milk exploitation is evident across mainland Europe. By contrast, the British Isles and western France maintain a gradual decline across 7,000 years after first evidence of milk about 5500 BC. Note that interpolation can colour some areas (particularly islands) for which no data are present.

in Methods). We found that patterns of milk usage provided no better explanation (no increased probability of observed allele frequency data) than assuming uniform selection in space and through time, contrary to the claims of others[33]. As an additional sensitivity test of this methodology, we tried using incident solar radiation as the main environmental variable driving LP selection intensity—in line with the calcium assimilation hypothesis[32]—and obtained higher probabilities of the observed allele frequency data (Extended Data Figs. 2 and 3 and Extended Data Table 1).

Health impacts of milk consumption

Our analysis of potsherd lipid residue and ancient LP allele data suggest that intensity of milk usage—beyond its mere presence—did not drive selection on LP. To explore other explanations for LP selection we first turned to contemporary data. The UK Biobank[4,5] includes genotypic and phenotypic data from about 500,000 people aged between 37 and 73 years, recruited between 2006 and 2010 (http://biobank.ndph.ox.ac.uk/showcase). In a subset of approximately 337,000 unrelated participants who classified themselves as 'white, British' and have similar genetic ancestry, LP genotypes were out of Hardy–Weinberg equilibrium (Extended Data Table 2), which could reflect genotype-related assortative mating[51] (for which there is weak evidence for LP; Extended Data Table 3), selection into a study or population structure, amongst other influences[52]. Around 92% (95% confidence interval (CI) 91.5–92.2%) of genetically LNP participants mainly use fresh cows' milk instead of soya or no milk (Table 1) and only 0.63% of milk consumers reported following a lactose-free diet (95% CI 0.59–0.67%). This suggests that LP has only a small effect on milk consumption and

use of lactose-free products is not an explanation. This finding is at odds with selection hypotheses of nutritional advantages from milk. Consistent with these results, some non-European countries with very low levels of LP have been importing milk in vast quantities in recent years as part of a more general adoption of Western diets. China, for example, has very low LP frequencies[31] and milk was rarely consumed in the early twentieth century[53] but milk consumption has increased more than 25-fold over the past five decades[54]. These findings bring into question the widely held belief that selection against LNP was the result of detrimental effects of milk consumption in otherwise healthy individuals—for example, through inducing stomach cramps, diarrhoea and flatulence[40,41,55–57]. One possible explanation for the small effect of LNP on milk intake in contemporary data is the use of mealtime lactase supplements that reduce symptoms of lactose intolerance. However, these have only become widely available recently and UK Biobank participants would not have had access to them for most of their lives.

We examined phenotypic associations of genetically predicted LP (Fig. 4) to investigate potential pathways through which selection could have occurred. The related calcium assimilation and vitamin D hypotheses[32] would anticipate LP to be associated with higher vitamin D concentration and bone mineral density due to its positive relationship with milk consumption[58–60]. However, these estimates are very close to the null and the large sample size puts considerable constraints on the magnitude of effects that could exist.

Milk consumption has been suggested to increase circulating insulin-like growth factor I (IGF-1)[61], leading others[62] to propose a model of LP selection driven by fitness advantages of IGF-1 acting to increase body size and lower age of sexual maturation. However, there were no meaningful differences in IGF-1 between LP and LNP individuals.
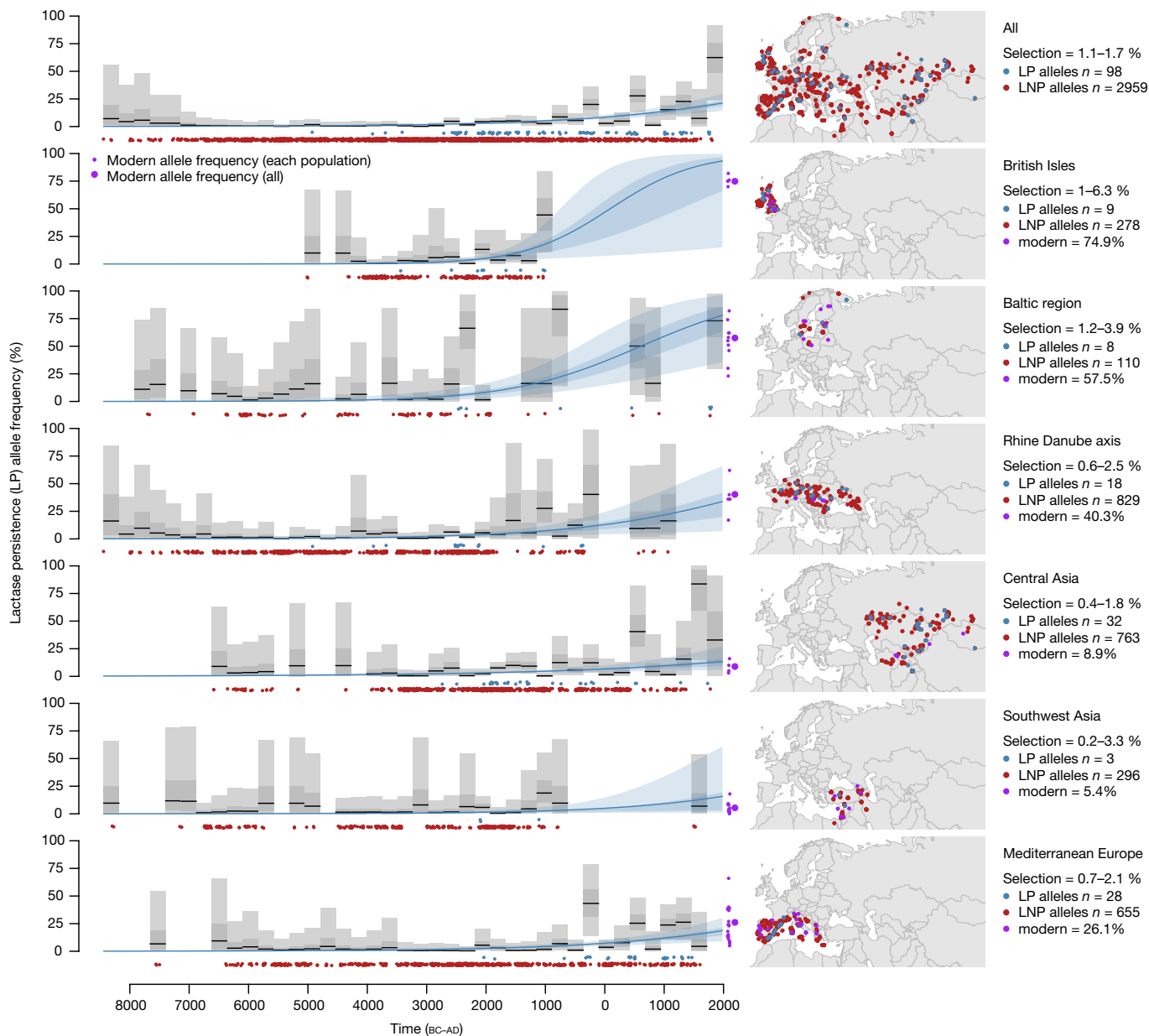
Fig. 3 | Regional variation in prehistoric LP allele frequencies in Europe. Observed aDNA data illustrated with blue and red dots showing the date and location of 3,057 LP and LNP alleles (rs4988235-A and rs4988235-G, respectively) from 1,770 ancient individuals. Grey bars and black lines show the 95%, 50% CI and MAP in time slices, using a Jeffreys prior. Slices with no observations remain blank. Blue lines illustrate maximum likelihood sigmoid curves of constant selection rate through time. Blue shading represents the 95%, 50% CI estimated from sigmoid joint parameters using Markov chain Monte Carlo methods. Likelihood function for sigmoid curves are constrained by three conservative prior beliefs to avoid absurd parameter combinations for regions with sparse data: (1) constant selection is <10% per 28 yr generation; (2) LP frequencies are <1% at 10000 BC; (3) LP frequencies are >1% at AD 2000. Small purple dots represent observed LP frequencies in modern populations in the same regions, as reported in supplementary data of ref. [31]; large purple dots represent a weighted average of these modern populations.

Nevertheless, LP allele presence was associated with 0.01 s.d. (95% CI 0.01, 0.02) higher body mass index (BMI), as previously reported[58–60] but not with height, consistent with other studies well controlled for population stratification[63,64]. Whilst statistically robust and replicating what has been observed in other large samples[58–60], the BMI effect is of small magnitude and congruent with a small difference in calorie intake consequent to milk consumption.

LP allele association with all-cause mortality, mother's age of death and father's age of death, were all close to the null. These results suggest that milk has little or no adverse health effect when consumed by LNP adults in a contemporary population. Another possible driver of selection is the influence of the LP allele on fertility but we found no meaningful effect of the LP allele presence on number of live births or number of children fathered.

Other drivers of LP evolution

Aside from dietary change, a number of other factors are likely to have influenced fecundity and mortality following the establishment of farming communities in Europe, including increased population and settlement density[65], increased mobility[66], proximity to animals, frequent crop failure, famine and population collapse[50] and general poor hygiene and sanitation. Most, if not all, of these factors are likely to have increased infectious disease loads, particularly zoonoses (about

Table 1 | Association of LP genotype and dairy milk intake

Genotype	Non-milk drinkers		Milk drinkers		Total	P value
GG— inferred LNP	1,646	8.1%	18,604	91.9%	20,250	
GA— inferred LP	8,374	6.8%	114,821	93.2%	123,195	
AA— inferred LP	12,672	6.7%	176,914	93.3%	189,586	
Total	22,692	6.8%	310,339	93.2%	333,031	8.5×10^{-14}

Unadjusted genotype association with self-reported milk preference (non-dairy, soya and never/rarely have milk versus dairy milk; derived from field 1418) in an unrelated white British subset of UK Biobank. The variant genotypes GG, GA and AA at locus rs4988235 produce lactase non-persistence (GG) and lactase persistence (GA/AA) phenotypes. Association P value was produced using the chi-squared test.

61% of known and about 75% of emerging human infectious disease today come from animals[67,68]). Given the widespread prehistoric exploitation of milk shown here (Fig. 2) and its relatively benign effects in healthy LNP individuals today, we propose two related mechanisms for the evolution of LP. First, as postulated in ref. [24], the detrimental health consequences of high-lactose food consumption by LNP individuals would be acutely manifested during famines, leading to high but episodic selection favouring LP. This is because lactose-induced diarrhoea can shift from an inconvenient to a fatal condition in severely malnourished individuals[69] and high-lactose (unfermented) milk products are more likely to be consumed when other food sources have been exhausted[70]. This we name the 'crisis mechanism', which predicts that LP selection pressures would have been greater during times of subsistence instability. A second mechanism relates to the increased pathogen loads—especially zoonoses—associated with farming and increased population density and mobility[66]. Mortality and morbidity due to pathogen exposure would have been amplified by the otherwise minor health effects of LNP in individuals consuming milk—particularly diarrhoea—due to fluid loss and other gut disturbances, leading to enhanced selection for LP[37]. We name this the 'chronic mechanism', which predicts that LP selection pressures would have increased with greater pathogen exposure. Crucially, proxies are available for some of the drivers of these suggested mechanisms, permitting us to explore the extent to which they explain LP selection and so allele frequency trajectories, using our maximum likelihood modelling approach. For the 'crisis mechanism' we use fluctuations in population size (residual fluctuations detrended for overall background growth) as a proxy for malnutrition exposure. For the 'chronic mechanism', we use temporal variation in settlement density as a proxy for pathogen exposure. Both proxies are constructed using an extensive database comprising >110,000 ^{14}C dates from >27,000 sites across the European and Mediterranean area. Model likelihoods (the probabilities of the allele frequency data; Extended Data Fig. 2) indicate that settlement density and population fluctuations both provide significantly (accounting for multiple testing via Benjamini–Hochberg; Extended Data Table 1) better explanations of LP allele frequency trajectories in prehistoric western Eurasia than do spatiotemporally uniform selection (Extended Data Figs. 4 and 5) or milk use, providing support for both the 'chronic' and 'crisis' mechanisms (the LP allele data are 284 or 689 times more probable under models of settlement density or population fluctuations, respectively, driving selection, than under a model of constant selection).

We also considered the proportion of domestic and wild animals in faunal assemblages—constructed using >1,000,000 NISPs (number of identified specimens) of 17 main meat-bearing taxa from 1,093 phases from 825 sites[49,71]—as explanatory variables for LP allele frequency trajectories. However, it is not clear if exploiting more domestic animals would increase pathogen exposure, as domesticates tend to live
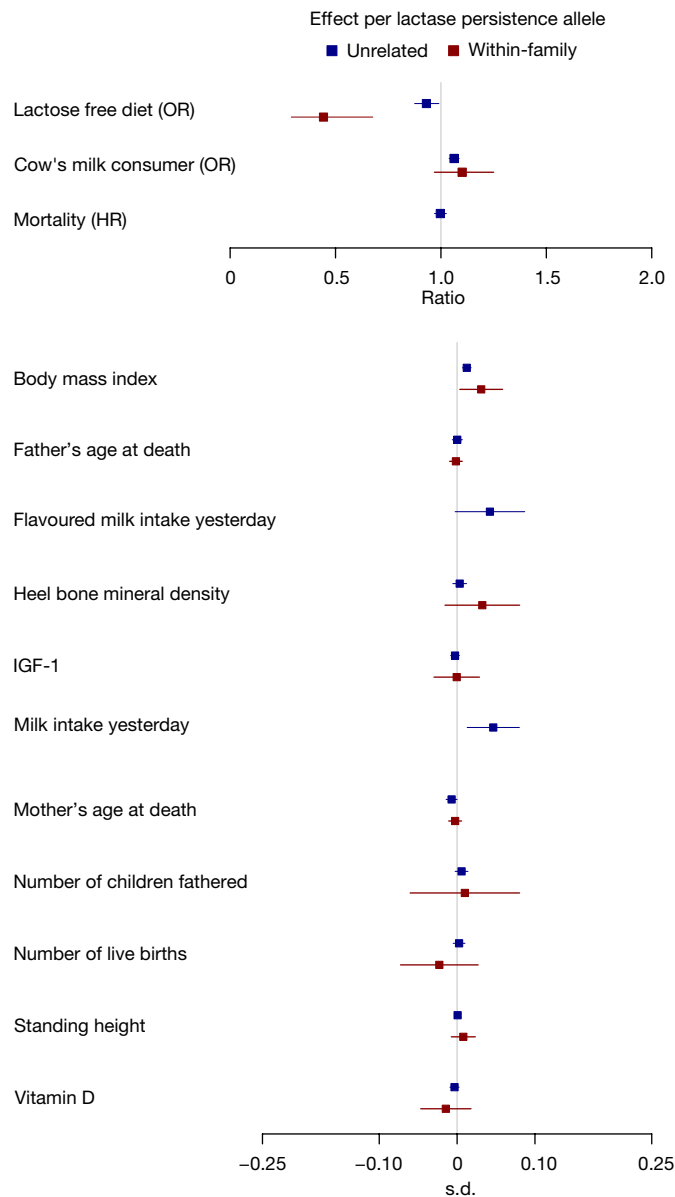

Fig. 4 | LP variant association with health outcomes. Variant associations with continuous (s.d. unit) or binary (odds ratio (OR), hazard ratio (HR)) outcomes adjusted for age, sex and top 40 genetic principal components. Unrelated estimates were produced using an unrelated white British subset of UK Biobank (n = 336,988): lactose-free diet (derived from field 20086; 0.95 OR (95% CI 0.89, 1.01)); cows' milk consumer (derived from field 1418; 1.06 OR (95% CI 1.04, 1.09)); mortality (derived from field 40000; 1.00 HR (95% CI 0.97, 1.03)); body mass index (field 21001; 0.01 s.d. (95% CI 0.01, 0.02)); father's age at death (field 1807; 2.35×10^{-4} s.d. (95% CI -6.27×10^{-3}, 6.74×10^{-3})); flavoured milk intake yesterday (field 100530; 0.04 s.d. (95% CI 0.00, 0.09)); heel bone mineral density (field 78; 3.31×10^{-3} s.d. (95% CI -5.52×10^{-3}, 0.01)); insulin-like growth factor 1 (IGF-1) (field 30770; -2.66×10^{-3} s.d. (95% CI -8.25×10^{-3}, 2.93×10^{-3})); milk intake yesterday (field 100520; 0.05 s.d. (95% CI 0.01, 0.08)); mother's age at death (field 3526; -0.01 s.d. (95% CI -0.01, -3.03×10^{-5})); number of children fathered (field 2405; 5.73×10^{-3} s.d. (95% CI -2.51×10^{-3}, 0.01)); number of live births (field 2734; 2.52×10^{-3} s.d. (95% CI -0.01, 0.01)); standing height (field 50; 6.37×10^{-4} s.d. (95% CI -3.22×10^{-3}, 4.49×10^{-3})); vitamin D (field 30890; -3.33×10^{-3} s.d. (95% CI -9.22×10^{-3}, 2.56×10^{-3})). Within-family estimates were produced using 40,273 siblings from 19,521 families. Within-family estimates of all-cause mortality, flavoured milk intake yesterday and milk intake yesterday could not be determined.

in closer proximity to humans than to wild animals[72], or if exploiting more wild animals would increase pathogen exposure, as greater pathogen diversity is expected for wild animals[73,74]. Furthermore,

a shift from domestic to wild animal exploitation might result from the economic instabilities associated with the 'crisis mechanism'[50,75]. Interestingly, the proportion of wild rather than domestic animals in archaeological assemblages provided higher model likelihoods (the LP allele data are 34 times more probable under a model of wild animal consumption driving selection, than a model of constant selection; Extended Data Fig. 6). This could be interpreted as support for either the 'crisis' or 'chronic' mechanisms or be argued to counter the 'chronic' mechanism if prehistoric pathogen exposure was mainly from domesticates.

The prevailing narrative for the coevolution of dairying and LP has been a virtuous circle mechanism in which LP frequency increased through the nutritional benefits and avoidance of negative health costs of milk consumption, facilitating an increasing reliance on milk that further drove LP selection. Our findings suggest a different picture. Milk consumption did not gradually grow throughout the European Neolithic period from initially low levels but rather was widespread at the outset in an almost entirely LNP population. We show that the scale of prehistoric milk use does not help to explain European LP allele frequency trajectories and thus it also cannot account for selection intensities. Furthermore, we show that LP status has little impact on modern milk consumption, mortality or fecundity and milk consumption has little or no detrimental health impact on contemporary healthy LNP individuals.

Instead, we find support for two related hypotheses: that LP selection was driven episodically and acutely by famine and/or on a more continuous basis by synergies between pathogen exposure and the otherwise benign consequences of milk consumption in LNP individuals[37]. We propose that these mechanisms would have applied in the disease- and malnutrition-prone environment existing during the period of rapid increase in LP frequency but would not be expected to apply outside these circumstances. This historical contingency is supported by the substantial increase in consumption of milk in contemporary China, where most of the population are LNP[76,77]. In contemporary populations, LP genotype associates strongly with aspects of the gut microbiome[78] but only in consumers of milk[79]. This suggests that when milk entered the diet of a LNP population it would have altered the gut microbiome. We postulate that, when combined with the changing pattern and prevalence of circulating infections consequent on increasing population density and settlement size, diarrhoeal disease mortality in late childhood could have been increased in LNP individuals drinking milk. Over the period in which LP prevalence increased, the ratio of late childhood (5–18 yr) to early childhood (2–5 yr) mortality increased[80]. The 'crisis' and 'chronic' mechanisms are, of course, not mutually exclusive, nor do they exclude other LP selection mechanisms, especially outside western Eurasia. We also test modern midday solar insolation incident on a horizontal surface[81] and our maximum likelihood approach does indeed provide support (see Extended Data Fig. 3) for the calcium assimilation hypothesis[32], although it should be noted that solar insolation is strongly correlated with latitude and may therefore be confounded by factors influencing the spatial spread of the LP allele, such as its origin location, 'allele surfing'[29,34] or large-scale population movements[26]. Other plausible proposals for selection favouring LP in Europe, such as milk as a relatively pathogen-free fluid[36], milk allowing earlier weaning and thus increased fertility[82], milk galacto-oligosaccharide benefits for the colonic microbiome[38,39] or higher efficiencies of calorie production from dairy farming[83] are more difficult to assess. However, we note that the best proxy for all of these processes is milk consumption level, which itself provides no better explanation for LP allele frequency trajectories than does constant selection through time. Therefore, the spatiotemporal patterns of LP selection in ancient Europeans probably do not reflect variation in their milk consumption. Instead, they map latitude, population volatility and settlement density—proxies for environmental conditions, subsistence economics and pathogen exposure, respectively. We note that—albeit in different configurations—these factors remain drivers of human morbidity and mortality today.

Online content

Any methods, additional references, Nature Research reporting summaries, source data, extended data, supplementary information, acknowledgements, peer review information; details of author contributions and competing interests; and statements of data and code availability are available at https://doi.org/10.1038/s41586-022-05010-7.

1. Sabeti, P. C. et al. Positive natural selection in the human lineage. *Science* **312**, 1614 (2006).
2. Evershed, R. P. et al. Earliest date for milk use in the Near East and southeastern Europe linked to cattle herding. *Nature* **455**, 528–531 (2008).
3. Debono Spiteri, C. et al. Regional asynchronicity in dairy production and processing in early farming communities of the northern Mediterranean. *Proc. Natl Acad. Sci. USA* **113**, 13594–13599 (2016).
4. Collins, R. What makes UK Biobank special? *Lancet* **379**, 1173–1174 (2012).
5. Allen, N. E., Sudlow, C., Peakman, T. & Collins, R. UK Biobank Data: come and get it. *Sci. Transl. Med.* **6**, 224ed224–224ed224 (2014).
6. Gerbault, P. et al. Evolution of lactase persistence: an example of human niche construction. *Philos. Trans. R. Soc. Lond. B* **366**, 863–877 (2011).
7. Food and Agriculture Organization of the United Nations. *Crops and Livestock Products (FAOSTAT)* http://www.fao.org/faostat/en/#data/QA (accessed 10 November 2021).
8. Vigne, J.-D. & Helmer, D. Was milk a "secondary product" in the Old World Neolithisation process? Its role in the domestication of cattle, sheep and goats. *Anthropozoologica* **42**, 9–40 (2007).
9. Roffet-Salque, M., Gillis, R., Evershed, R. P. & Vigne, J.-D. in *Hybrid Communities: Biosocial Approaches to Domestication and Other Trans-Species Relationships* (eds Stépanoff, C. & Vigne, J.D.) 127–143 (Routledge, 2018).
10. Gillis, R. et al. Sophisticated cattle dairy husbandry at Borduşani-Popină (Romania, fifth millennium BC): the evidence from complementary analysis of mortality profiles and stable isotopes. *World Archaeol.* **45**, 447–472 (2013).
11. Ethier, J. et al. Earliest expansion of animal husbandry beyond the Mediterranean zone in the sixth millennium BC. *Sci. Rep.* **7**, 7146 (2017).
12. Salque, M. et al. Earliest evidence for cheese making in the sixth millennium BC in northern Europe. *Nature* **493**, 522–525 (2013).
13. Gillis, R. E. et al. The evolution of dual meat and milk cattle husbandry in Linearbandkeramik societies. *Proc. R. Soc. B* **284**, 20170905 (2017).
14. Balasse, M. & Tresset, A. Early weaning of Neolithic domestic cattle (Bercy, France) revealed by intra-tooth variation in nitrogen isotope ratios. *J. Archaeol. Sci.* **29**, 853–859 (2002).
15. Whelton, H. L., Roffet-Salque, M., Kotsakis, K., Urem-Kotsou, D. & Evershed, R. P. Strong bias towards carcass product processing at Neolithic settlements in northern Greece revealed through absorbed lipid residues of archaeological pottery. *Quat. Int.* **496**, 127–139 (2018).
16. Copley, M. S. et al. Direct chemical evidence for widespread dairying in prehistoric Britain. *Proc. Natl Acad. Sci. USA* **100**, 1524–1529 (2003).
17. Cramp, L. J. E. et al. Immediate replacement of fishing with dairying by the earliest farmers of the northeast Atlantic archipelagos. *Proc. R. Soc. B* **281**, 20132372 (2014).
18. Smyth, J. & Evershed, R. P. Milking the megafauna: using organic residue analysis to understand early farming practice. *Environ. Archaeol.* **21**, 214–229 (2016).
19. Charlton, S. et al. New insights into Neolithic milk consumption through proteomic analysis of dental calculus. *Archaeol. Anthropol. Sci.* **11**, 6183–6196 (2019).
20. Craig, O. E. et al. Ancient lipids reveal continuity in culinary practices across the transition to agriculture in Northern Europe. *Proc. Natl Acad. Sci. USA* **108**, 17910–17915 (2011).
21. Cramp, L. J. E. et al. Neolithic dairy farming at the extreme of agriculture in Northern Europe. *Proc. R. Soc. B* **281**, 20140819 (2014).
22. Pääkkönen, M., Holmqvist, E., Bläuer, A., Evershed, R. P. & Asplund, H. Diverse economic patterns in the North Baltic Sea region in the Late Neolithic and Early Metal periods. *Eur. J. Archaeol.* **23**, 4–21 (2019).
23. Burger, J., Kirchner, M., Bramanti, B., Haak, W. & Thomas, M. G. Absence of the lactase-persistence-associated allele in early Neolithic Europeans. *Proc. Natl Acad. Sci. USA* **104**, 3736–3741 (2007).
24. Sverrisdóttir, O. Ó. et al. Direct estimates of natural selection in Iberia indicate calcium absorption was not the only driver of lactase persistence in Europe. *Mol. Biol. Evol.* **31**, 975–983 (2014).
25. Allentoft, M. E. et al. Population genomics of Bronze Age Eurasia. *Nature* **522**, 167–172 (2015).
26. Haak, W. et al. Massive migration from the steppe was a source for Indo-European languages in Europe. *Nature* **522**, 207–211 (2015).
27. Brace, S. et al. Ancient genomes indicate population replacement in Early Neolithic Britain. *Nat. Ecol. Evol.* **3**, 765–771 (2019).
28. Burger, J. et al. Low prevalence of lactase persistence in Bronze Age Europe indicates ongoing strong selection over the last 3,000 years. *Curr. Biol.* **30**, 4307–4315 (2020).
29. Itan, Y., Powell, A., Beaumont, M. A., Burger, J. & Thomas, M. G. The origins of lactase persistence in Europe. *PLoS Comput. Biol.* **5**, e1000491 (2009).
30. Enattah, N. S. et al. Identification of a variant associated with adult-type hypolactasia. *Nat. Genet.* **30**, 233–237 (2002).
31. Itan, Y., Jones, B., Ingram, C., Swallow, D. & Thomas, M. A worldwide correlation of lactase persistence phenotype and genotypes. *BMC Evol. Biol.* **10**, 36 (2010).
32. Flatz, G. & Rotthauwe, H. Lactose nutrition and natural selection. *Lancet* **302**, 76–77 (1973).

Article

33. Cubas, M. et al. Latitudinal gradient in dairy production with the introduction of farming in Atlantic Europe. *Nat. Commun.* **11**, 2036 (2020).
34. Klopfstein, S., Currat, M. & Excoffier, L. The fate of mutations surfing on the wave of a range expansion. *Mol. Biol. Evol.* **23**, 482–490 (2006).
35. Gerbault, P., Moret, C., Currat, M. & Sanchez-Mazas, A. Impact of selection and demography on the diffusion of lactase persistence. *PLoS ONE* **4**, e6369 (2009).
36. Cook, G. C. & al-Torki, M. T. High intestinal lactase concentrations in adult Arabs in Saudi Arabia. *Br. Med. J.* **3**, 135–136 (1975).
37. Davey Smith, G. et al. Lactase persistence-related genetic variant: population substructure and health outcomes. *Eur. J. Hum. Genet.* **17**, 357–367 (2009).
38. Cederlund, A. et al. Lactose in human breast milk an inducer of innate immunity with implications for a role in intestinal homeostasis. *PLoS ONE* https://doi.org/10.1371/journal.pone0053876 (2013).
39. Gibson, P. R. History of the low FODMAP diet. *J. Gastroenterol. Hepatol.* **32**, 5–7 (2017).
40. Walker, C. & Thomas, M. G. in *Lactose: Evolutionary Role, Health Effects, and Applications* (eds Paques, M. & Lindner, C.) 1–48 (Elsevier, 2019).
41. Simoons, F. Primary adult lactose intolerance and the milking habit: a problem in biologic and cultural interrelations. II. A culture historical hypothesis. *Dig. Dis. Sci.* **15**, 695–710 (1970).
42. McCracken, R. D. Lactase deficiency: an example of dietary evolution. *Curr. Anthropol.* **12**, 479–517 (1971).
43. Holden, C. & Mace, R. Phylogenetic analysis of the evolution of lactose digestion in adults. *Hum. Biol.* **69**, 605–628 (1997).
44. Ingram, C. J. E. et al. A novel polymorphism associated with lactose tolerance in Africa: multiple causes for lactase persistence? *Hum. Genet.* **120**, 779–788 (2007).
45. Tishkoff, S. A. et al. Convergent adaptation of human lactase persistence in Africa and Europe. *Nat. Genet.* **39**, 31–40 (2007).
46. Joslin, S. E. K. et al. Association of the lactase persistence haplotype block with disease risk in populations of European descent. *Front. Genet.* **11**, 1346 (2020).
47. Dudd, S. N. & Evershed, R. P. Direct demonstration of milk as an element of archaeological economies. *Science* **282**, 1478–1481 (1998).
48. Dunne, J. et al. First dairying in green Saharan Africa in the fifth millennium BC. *Nature* **486**, 390–394 (2012).
49. Manning, K. et al. The origins and spread of stock-keeping: the role of cultural and environmental influences on early Neolithic animal exploitation in Europe. *Antiquity* **87**, 1046–1059 (2013).
50. Shennan, S. et al. Regional population collapse followed initial agriculture booms in mid-Holocene Europe. *Nat. Commun.* **4**, 2486 (2013).
51. Howe, L. J. et al. Genetic evidence for assortative mating on alcohol consumption in the UK Biobank. *Nat. Commun.* **10**, 5039 (2019).
52. Rodriguez, S., Gaunt, T. R. & Day, I. N. M. Hardy–Weinberg equilibrium testing of biological ascertainment for Mendelian randomization studies. *Am. J. Epidemiol.* **169**, 505–514 (2009).
53. Simmons, J. S., Whayne, T. F., Anderson, G. W. & Horack, H. M. *Global Epidemiology: A Geography of Disease and Sanitation* Vol. 1 (William Heineman, 1944).
54. Bai, Z. et al. Global environmental costs of China's thirst for milk. *Glob. Change Biol.* **24**, 2198–2211 (2018).
55. Simoons, F. Primary adult lactose intolerance and the milking habit: a problem in biological and cultural interrelations. I. Review of the medical research. *Dig. Dis. Sci.* **14**, 819–836 (1969).
56. Bayless, T. M., Paige, D. M. & Ferry, G. D. Lactose intolerance and milk drinking habits. *Gastroenterology* **60**, 605–608 (1971).
57. Szilagyi, A., Walker, C. & Thomas, M. G. in *Lactose: Evolutionary Role, Health Effects, and Applications* (eds Paques, M. & Lindner, C.) 113–153 (Elsevier, 2019).
58. Mendelian Randomization of Dairy Consumption Working Group. Dairy consumption and body mass index among adults: Mendelian randomization analysis of 184802 individuals from 25 studies. *Clin. Chem.* **64**, 183–191 (2018).
59. Almon, R., Álvarez-León, E. E. & Serra-Majem, L. Association of the European lactase persistence variant (LCT-13910 C>T polymorphism) with obesity in the Canary Islands. *PLoS ONE* https://doi.org/10.1371/journal.pone.0043978 (2012).
60. Hartwig, F. P., Horta, B. L., Davey Smith, G., de Mola, C. L. & Victora, C. G. Association of lactase persistence genotype with milk consumption, obesity and blood pressure: a Mendelian randomization study in the 1982 Pelotas (Brazil) Birth Cohort, with a systematic review and meta-analysis. *Int. J. Epidemiol.* **45**, 1573–1587 (2016).
61. Qin, L.-Q., He, K. & Xu, J.-Y. Milk consumption and circulating insulin-like growth factor-I level: a systematic literature review. *Int. J. Food Sci. Nutr.* **60**, 330–340 (2009).
62. Wiley, A. The evolution of lactase persistence: milk consumption, insulin-like growth factor I, and human life-history parameters. *Q. Rev. Biol.* **93**, 319–345 (2018).
63. Campbell, C. D. et al. Demonstrating stratification in a European American population. *Nat. Genet.* **37**, 868–872 (2005).
64. Bergholdt, H. K. M., Nordestgaard, B. G., Varbo, A. & Ellervik, C. Milk intake is not associated with ischaemic heart disease in observational or Mendelian randomization analyses in 98,529 Danish adults. *Int. J. Epidemiol.* **44**, 587–603 (2015).
65. Bocquet-Appel, J.-P. When the world's population took off: the springboard of the Neolithic demographic transition. *Science* **333**, 560–561 (2011).
66. Loog, L. et al. Estimating mobility using sparse data: application to human genetic variation. *Proc. Natl Acad. Sci. USA* **114**, 12213–12218 (2017).
67. Vorou, R., Papavassiliou, V. & Tsiodras, S. Emerging zoonoses and vector-borne infections affecting humans in Europe. *Epidemiol. Infect.* **135**, 1231–1247 (2007).
68. Allen, T. et al. Global hotspots and correlates of emerging zoonotic diseases. *Nat. Commun.* **8**, 1124 (2017).
69. Rice, A. L., Sacco, L., Hyder, A. & Black, R. E. Malnutrition as an underlying cause of childhood deaths associated with infectious diseases in developing countries. *Bull. World Health Org.* **78**, 1207–1221 (2000).
70. Colledge, S., Conolly, J., Crema, E. & Shennan, S. Neolithic population crash in northwest Europe associated with agricultural crisis. *Quat. Res.* **92**, 686–707 (2019).
71. Manning, K. The cultural evolution of Neolithic Europe. EUROEVOL Dataset 2: Zooarchaeological data. *J. Open Archaeol. Data* **5**, e3 (2016).
72. Chessa, B. et al. Revealing the history of sheep domestication using retrovirus integrations. *Science* **324**, 532 (2009).
73. Karesh, W. B., Cook, R. A., Bennett, E. L. & Newcomb, J. Wildlife trade and global disease emergence. *Emerg. Infect. Dis.* **11**, 1000 (2005).
74. Chomel, B. B., Belotto, A. & Meslin, F.-X. Wildlife, exotic pets, and emerging zoonoses. *Emerg. Infect. Dis.* **13**, 6 (2007).
75. Schibler, J., Jacomet, S., Hüster-Plogmann, H. & Brombacher, C. Economic crash in the 37th and 36th centuries cal. BC in Neolithic lake shore sites in Switzerland. *Anthropozoologica* **25**, 553–570 (1997).
76. He, Y., Yang, X., Xia, J., Zhao, L. & Yang, Y. Consumption of meat and dairy products in China: a review. *Proc. Nutr. Soc.* **75**, 385–391 (2016).
77. Mak, V. S. W. *Milk Craze: Body, Science, and Hope in China* (Univ. of Hawai'i Press, 2021).
78. Goodrich, J. K. et al. Genetic determinants of the gut microbiome in UK twins. *Cell Host Microbe* **19**, 731–743 (2016).
79. Qin, Y. et al. Combined effects of host genetics and diet on human gut microbiota and incident disease in a single population cohort. *Nat. Genet.* **54**, 134–142 (2022).
80. Paine, R. R. & Boldsen, J. L. in *The Evolution of Human Life History School for Advanced Research* (eds Hawkes, K. & Paine, R. R.) 307–330 (School of American Research Press, 2006).
81. Stackhouse P. W. et al. *POWER Release 8.0.1 (with GIS Applications) Methodology (Data Parameters, Sources, & Validation)* (NASA, 2018).
82. Lieberman, M. & Lieberman, D. Lactase deficiency: a genetic mechanism which regulates the time of weaning. *Am. Nat.* **112**, 625–627 (1978).
83. Ingold, T. *Hunters, Pastoralists and Ranchers: Reindeer Economies and Their Transformations* (Cambridge Univ. Press, 1980).
84. Outram, A. K. et al. The earliest horse harnessing and milking. *Science* **323**, 1332–1335 (2009).
85. Breu, A., Gómez-Bach, A., Heron, C., Rosell-Melé, A. & Molist, M. Variation in pottery use across the Early Neolithic in the Barcelona plain. *Archaeol. Anthropol. Sci.* **13**, 53 (2021).
86. Brychova, V. et al. Animal exploitation and pottery use during the early LBK phases of the Neolithic site of Bylany (Czech Republic) tracked through lipid residue analysis. *Quat. Int.* **574**, 91–101 (2021).
87. Carrer, F. et al. Chemical analysis of pottery demonstrates prehistoric origin for high-altitude alpine dairying. *PLoS ONE* **11**, e0151442 (2016).
88. Casanova, E. et al. Spatial and temporal disparities in human subsistence in the Neolithic Rhineland gateway. *J. Archaeol. Sci.* **122**, 105215 (2020).
89. Colonese, A. C. et al. The identification of poultry processing in archaeological ceramic vessels using in-situ isotope references for organic residue analysis. *J. Archaeol. Sci.* **78**, 179–192 (2017).
90. Copley, M. S. et al. Dairying in antiquity. I. Evidence from absorbed lipid residues dating to the British Iron Age. *J. Archaeol. Sci.* **32**, 485–503 (2005).
91. Copley, M. S., Berstan, R., Straker, V., Payne, S. & Evershed, R. P. Dairying in antiquity. II. Evidence from absorbed lipid residues dating to the British Bronze Age. *J. Archaeol. Sci.* **32**, 505–521 (2005).
92. Copley, M. S. et al. Dairying in antiquity. III. Evidence from absorbed lipid residues dating to the British Neolithic. *J. Archaeol. Sci.* **32**, 523–546 (2005).
93. Copley, M. S. & Evershed, R. P. in *Building Memories: the Neolithic Cotswold Long Barrow at Ascott-under-Wychwood, Oxfordshire* (eds Benson, D. & Whittle, A.) 283–288 (Oxbow Books, 2006).
94. Courel, B. et al. Organic residue analysis shows sub-regional patterns in the use of pottery by Northern European hunter–gatherers. *R. Soc. Open Sci.* **7**, 192016 (2020).
95. Craig, O. E. et al. Did the first farmers of central and eastern Europe produce dairy foods? *Antiquity* **79**, 882–894 (2005).
96. Craig, O. E., Taylor, G., Mulville, J., Collins, M. J. & Parker Pearson, M. The identification of prehistoric dairying activities in the Western Isles of Scotland: an integrated biomolecular approach. *J. Archaeol. Sci.* **32**, 91–103 (2005).
97. Craig, O. E. et al. Molecular and isotopic demonstration of the processing of aquatic products in Northern European Prehistoric pottery. *Archaeometry* **49**, 135–152 (2007).
98. Craig, O. in *Archaeology Meets science: Biomolecular Investigations in Bronze Age Greece* (eds Tzedakis, Y. et. al.) 121–124 (Oxbow Books, 2008).
99. Craig, O. E. et al. Feeding Stonehenge: cuisine and consumption at the Late Neolithic site of Durrington Walls. *Antiquity* **89**, 1096–1109 (2015).
100. Craig-Atkins, E. et al. The dietary impact of the Norman Conquest: a multiproxy archaeological investigation of Oxford, UK. *PLoS ONE* **15**, e0235005 (2020).
101. Cramp, L. J. E., Evershed, R. P. & Eckardt, H. What was a mortarium used for? Organic residues and cultural change in Iron Age and Roman Britain. *Antiquity* **85**, 1339–1352 (2011).
102. Cramp, L. J. E. et al. Regional diversity in subsistence among early farmers in Southeast Europe revealed by archaeological organic residues. *Proc. R. Soc. B* **286**, 20182347 (2019).
103. Cramp, L. J. E., Król, D., Rutter, M., Heyd, V. M. & Pospieszny, L. Analiza pozostałości organicznych z ceramiki kultury rzucewskiej z Rzucewa. *Pomorania Antiqua* **XXVIII**, 245–259 (2019).
104. Demirci, Ö., Lucquin, A., Craig, O. E. & Raemaekers, D. C. M. First lipid residue analysis of Early Neolithic pottery from Swifterbant (the Netherlands, ca. 4300–4000 BC). *Archaeol. Anthropol. Sci.* **12**, 105 (2020).
105. Demirci, Ö., Lucquin, A., Çakırlar, C., Craig, O. E. & Raemaekers, D. C. M. Lipid residue analysis on Swifterbant pottery (c. 5000–3800 cal BC) in the Lower Rhine–Meuse area (the Netherlands) and its implications for human–animal interactions in relation to the Neolithisation process. *J. Archaeol. Sci. Rep.* **36**, 102812 (2021).
106. Dreslerová, D. et al. Seeking the meaning of a unique mountain site through a multidisciplinary approach. The Late La Tène site at Sklářské Valley, Šumava Mountains, Czech Republic. *Quat. Int.* **542**, 88–108 (2020).

107. Drieu, L. et al. Chemical evidence for the persistence of wine production and trade in Early Medieval Islamic Sicily. *Proc. Natl Acad. Sci. USA* **118**, e2017983118 (2021).

108. Drieu, L. et al. A Neolithic without dairy? Chemical evidence from the content of ceramics from the Pendimoun rock-shelter (Castellar, France, 5750–5150 BC). *J. Archaeol. Sci. Rep.* **35**, 102682 (2021).

109. Dunne, J. et al. Milk of ruminants in ceramic baby bottles from prehistoric child graves. *Nature* **574**, 246–248 (2019).

110. Dunne, J., Chapman, A., Blinkhorn, P. & Evershed, R. P. Reconciling organic residue analysis, faunal, archaeobotanical and historical records: diet and the medieval peasant at West Cotton, Rautis, Northamptonshire. *J. Archaeol. Sci.* **107**, 58–70 (2019).

111. Dunne, J., Chapman, A., Blinkhorn, P. & Evershed, R. P. Fit for purpose? Organic residue analysis and vessel specialisation: the perfectly utilitarian medieval pottery assemblage from West Cotton, Rautis. *J. Archaeol. Sci.* **120**, 105178 (2020).

112. Dunne, J. et al. Finding Oxford's medieval Jewry using organic residue analysis, faunal records and historical documents. *Archaeol. Anthropol. Sci.* **13**, 48 (2021).

113. Evershed, R. P., Copley, M. S., Dickson, L. & Hansel, F. A. Experimental evidence for the processing of marine animal products and other commodities containing polyunsaturated fatty acids in pottery vessels. *Archaeometry* **50**, 101–113 (2008).

114. Fanti, L. et al. The role of pottery in Middle Neolithic societies of western Mediterranean (Sardinia, Italy, 4500–4000 cal BC) revealed through an integrated morphometric, use-wear, biomolecular and isotopic approach. *J. Archaeol. Sci.* **93**, 110–128 (2018).

115. Francés-Negro, M. et al. Neolithic to Bronze Age economy and animal management revealed using analyses of lipid residues of pottery vessels and faunal remains at El Portalón de Cueva Mayor (Sierra de Atapuerca, Spain). *J. Archaeol. Sci.* **131**, 105380 (2021).

116. Gregg, M. W., Banning, E. B., Gibbs, K. & Slater, G. F. Subsistence practices and pottery use in Neolithic Jordan: molecular and isotopic evidence. *J. Archaeol. Sci.* **36**, 937–946 (2009).

117. Gunnarsone, A., Oras, E., Talbot, H. M., Ilves, K. & Legzdiņa, D. Cooking for the living and the dead: lipid residues of Rauši settlement and cemetery pottery from the 11th–13th century. *Estonian J. Archaeol.* **24**, 45–69 (2020).

118. Heron, C. et al. Cooking fish and drinking milk? Patterns in pottery use in the southeastern Baltic, 3300–2400 cal BC. *J. Archaeol. Sci.* **63**, 33–43 (2015).

119. Hoekman-Sites, H. A. & Giblin, J. I. Prehistoric animal use on the Great Hungarian Plain: a synthesis of isotope and residue analyses from the Neolithic and Copper Age. *J. Anthropol. Archaeol.* **31**, 515–527 (2012).

120. Isaksson, S. & Hallgren, F. Lipid residue analyses of Early Neolithic funnel-beaker pottery from Skogsmossen, eastern Central Sweden, and the earliest evidence of dairying in Sweden. *J. Archaeol. Sci.* **39**, 3600–3609 (2012).

121. Krueger, M., Bajčev, O., Whelton, H. L. & Evershed, R. P. in *The Neolithic in the Middle Morava Valley* (ed. Perić, S.) Vol. 3, 61–76 (Institute of Archaeology, 2019).

122. Manzano, E. et al. An integrated multianalytical approach to the reconstruction of daily activities at the Bronze Age settlement in Peñalosa (Jaén, Spain). *Microchem. J.* **122**, 127–136 (2015).

123. Manzano, E. et al. Molecular and isotopic analyses on prehistoric pottery from the Virués-Martínez cave (Granada, Spain). *J. Archaeol. Sci. Rep.* **27**, 101929 (2019).

124. Matlova, V. et al. Defining pottery use and animal management at the Neolithic site of Bylany (Czech Republic). *J. Archaeol. Sci. Rep.* **14**, 262–274 (2017).

125. McClure, S. B. et al. Fatty acid specific $\delta^{13}C$ values reveal earliest Mediterranean cheese production 7,200 years ago. *PLoS ONE* **13**, e0202807 (2018).

126. Mileto, S., Kaiser, E., Rassamakin, Y., Whelton, H. & Evershed, R. P. Differing modes of animal exploitation in North-Pontic Eneolithic and Bronze Age Societies. *Sci. Technol. Archaeol. Res.* **3**, 112–125 (2017).

127. Mukherjee, A. J., Berstan, R., Copley, M. S., Gibson, A. M. & Evershed, R. P. Compound-specific stable carbon isotopic detection of pig product processing in British Late Neolithic pottery. *Antiquity* **83**, 743–754 (2007).

128. Mukherjee, A. J., Gibson, A. M. & Evershed, R. P. Trends in pig product processing at British Neolithic Grooved Ware sites traced through organic residues in potsherds. *J. Archaeol. Sci.* **35**, 2059–2073 (2008).

129. Ogrinc, N., Budja, M., Potočnik, D., Žibrat Gašparič, A. & Mlekuž, D. Lipids, pots and food processing at Hočevarica, Ljubljansko barje, Slovenia. *Doc. Praehist.* **XLI**, 181–194 (2014).

130. Oras, E. et al. The adoption of pottery by north-east European hunter-gatherers: evidence from lipid residue analysis. *J. Archaeol. Sci.* **78**, 112–119 (2017).

131. Oras, E. et al. Social food here and hereafter: multiproxy analysis of gender-specific food consumption in conversion period inhumation cemetery at Kukruse, NE-Estonia. *J. Archaeol. Sci.* **97**, 90–101 (2018).

132. Outram, A. K. et al. Horses for the dead: funerary foodways in Bronze Age Kazakhstan. *Antiquity* **85**, 116–128 (2011).

133. Outram, A. K. et al. Patterns of pastoralism in later Bronze Age Kazakhstan: new evidence from faunal and lipid residue analyses. *J. Archaeol. Sci.* **39**, 2424–2435 (2012).

134. Özbal, H. et al. Neolitik Batı Anadolu ve Marmara yerleşimleri çanak çömleklerinde organik kalıntı analizleri. *Arkeometri Sonuçları Toplantısı* **28**, 105–114 (2013).

135. Özbal, H. et al. Yenikapı, Aşağıpınar, Bademağacı ve Barcın Çömleklerindeorganik kalıntı analizi. *Arkeometri Sonuçları Toplantısı* **29**, 83–90 (2013).

136. Pääkkönen, M., Bläuer, A., Evershed, R. P. & Asplund, H. Reconstructing food procurement and processing in early Comb ware period through organic residues in early Comb and Jäkärlä ware pottery. *Fennosc. Archaeol.* **XXXIII**, 57–75 (2016).

137. Pääkkönen, M., Bläuer, A., Olsen, B., Evershed, R. P. & Asplund, H. Contrasting patterns of prehistoric human diet and subsistence in northernmost Europe. *Sci. Rep.* **8**, 1148 (2018).

138. Papakosta, V., Oras, E. & Isaksson, S. Early pottery use across the Baltic—a comparative lipid residue study on Ertebølle and Narva ceramics from coastal hunter-gatherer sites in southern Scandinavia, northern Germany and Estonia. *J. Archaeol. Sci. Rep.* **24**, 142–151 (2019).

139. Pennetta, A., Fico, D., Lucrezia Savino, M., Larocca, F. & Egidio De Benedetto, G. Characterization of Bronze age pottery from the Grotte di Pertosa-Auletta (Italy): results from the first analysis of organic lipid residues. *J. Archaeol. Sci. Rep.* **31**, 102308 (2020).

140. Piličiauskas, G. et al. The Corded Ware culture in the Eastern Baltic: new evidence on chronology, diet, beaker, bone and flint tool function. *J. Archaeol. Sci. Rep.* **21**, 538–552 (2018).

141. Piličiauskas, G. et al. Fishers of the Corded Ware culture in the Eastern Baltic. *Acta Archaeol.* **91**, 95–120 (2020).

142. Robinson, G. et al. Furness's first farmers: evidence of Early Neolithic settlement and dairying in Cumbria. *Proc. Prehist. Soc.* **86**, 165–198 (2020).

143. Robson, H. K. et al. Diet, cuisine and consumption practices of the first farmers in the southeastern Baltic. *Archaeol. Anthropol. Sci.* **11**, 4011–4024 (2019).

144. Roffet-Salque, M. & Evershed, R. P. in *Kopydłowo, stanowisko 6. Osady neolityczne z pogranicza Kujaw i Wielkopolski* (eds Marciniak, A. et al.) 133–142 (Wydawnictwo Profil-Archeo, 2015).

145. Roffet-Salque, M., Banecki, B. & Evershed, R. P. in *A Megalithic Tomb of the Globular Amphora Culture from Kierzkowo in the Pałuki Region—A Silent Witness of Ancestor Worship from the Stone Age Biskupin Archaeological Works* (eds Nowaczyk, S. et al.) 251–266 (Archaeological Museum in Biskupin, 2017).

146. Roffet-Salque, M. et al. in *Ludwinowo 7—Neolithic Settlement in Kuyavia Saved Archaeological Heritage* 8 (Joanna Pyzel, J.) 301–316 (Profil-Archeo Publishing House and Archaeological Studio, University of Gdańsk Publishing House, 2019).

147. Salque, M. et al. New insights into the early Neolithic economy and management of animals in Southern and Central Europe revealed using lipid residue analyses of pottery vessels. *Anthropozoologica* **47**, 45–61 (2012).

148. Smyth, J. & Evershed, R. P. The molecules of meals: new insight into Neolithic foodways. *Proc. R. Ir. Acad.* **115C**, 27–46 (2015).

149. Šoberl, L. *Pots for the Afterlife: Organic Residue Analysis of British Early Bronze Age Pottery from Funerary Contexts.* PhD thesis. Univ. of Bristol (2011).

150. Šoberl, L., Žibrat Gašparič, A., Budja, M. & Evershed, R. P. Early herding practices revealed through organic residue analysis of pottery from the early Neolithic rock shelter of Mala Triglavca, Slovenia. *Doc. Praehist.* **35**, 253–260 (2008).

151. Šoberl, L. et al. Neolithic and Eneolithic activities inferred from organic residue analysis of pottery from Mala Triglavca, Moverna vas and Ajdovska jama, Slovenia. *Doc. Praehist.* **XLI**, 149–179 (2014).

152. Spangenberg, J. E., Jacomet, S. & Schibler, J. Chemical analyses of organic residues in archaeological pottery from Arbon Bleiche 3, Switzerland—evidence for dairying in the late Neolithic. *J. Archaeol. Sci.* **33**, 1–13 (2006).

153. Spangenberg, J. E., Matuschik, I., Jacomet, S. & Schibler, J. Direct evidence for the existence of dairying farms in prehistoric Central Europe (4th mil. BC). *Isotopes Environ. Health Stud.* **44**, 189–200 (2008).

154. Spataro, M. et al. Production and function of Neolithic black-painted pottery from Schela Cladovei (Iron Gates, Romania). *Archaeol. Anthropol. Sci.* **11**, 6287–6304 (2019).

155. Steele, V. J. & Stern, B. Red Lustrous Wheelmade ware: analysis of organic residues in Late Bronze Age trade and storage vessels from the eastern Mediterranean. *J. Archaeol. Sci. Rep.* **16**, 641–657 (2017).

156. Stojanovski, D. et al. Living off the land: terrestrial-based diet and dairying in the farming communities of the Neolithic Balkans. *PLoS ONE* **15**, e0237608 (2020).

157. Stojanovski, D. et al. Anta 1 de Val da Laje—the first direct view at diet, dairying practice and socio-economic aspects of pottery use in the final Neolithic of central Portugal. *Quat. Int.* **542**, 1–8 (2020).

158. Tarifa-Mateo, N. et al. New insights from Neolithic pottery analyses reveal subsistence practices and pottery use in early farmers from Cueva de El Toro (Málaga, Spain). *Archaeol. Anthropol. Sci.* **11**, 5199–5211 (2019).

159. Weber, J., Brozio, J. P., Müller, J. & Schwark, L. Grave gifts manifest the ritual status of cattle in Neolithic societies of northern Germany. *J. Archaeol. Sci.* **117**, 105122 (2020).

160. Evershed, R. P., Heron, C. & Goad, L. J. Analysis of organic residues of archaeological origin by high-temperature gas chromatography and gas chromatography-mass spectrometry. *Analyst* **115**, 1339–1342 (1990).

161. Correa-Ascencio, M. & Evershed, R. P. High throughput screening of organic residues in archaeological potsherds using direct methanolic acid extraction. *Anal. Methods* **6**, 1330–1340 (2014).

162. Reimer, P. J. et al. IntCal13 and Marine13 radiocarbon age calibration curves 0–50,000 years cal BP. *Radiocarbon* **55**, 1869–1887 (2013).

163. Bronk Ramsey, C. Bayesian analysis of radiocarbon dates. *Radiocarbon* **51**, 337–360 (2009).

164. Graffelman, J. Exploring diallelic genetic markers: the HardyWeinberg package. *J. Stat. Softw.* **64**, 1–23 (2015).

165. Karczewski, K. J. et al. The mutational constraint spectrum quantified from variation in 141,456 humans. *Nature* **581**, 434–443 (2020).

166. Mitchell, R., Hemani, G., Dudding, T. & Paternoster, L. *UK Biobank Genetic Data: MRC-IEU Quality Control* Version 2; https://doi.org/10.5523/bris.1ovaau5sxunp2cv8rcy88688v (Univ. Bristol, 2019).

167. Brumpton, B. et al. Avoiding dynastic, assortative mating, and population stratification biases in Mendelian randomization through within-family analyses. *Nat. Commun.* **11**, 3519 (2020).

168. Howe, L. J. et al. Within-sibship genome-wide association analyses decrease bias in estimates of direct genetic effects. *Nat. Genet.* **54**, 581–592 (2022).

169. Agranat-Tamir, L. et al. The genomic history of the Bronze Age Southern Levant. *Cell* **181**, 1146–1157 (2020).

170. Antonio, M. L. et al. Ancient Rome: a genetic crossroads of Europe and the Mediterranean. *Science* **366**, 708–714 (2019).

171. Broushaki, F. et al. Early Neolithic genomes from the eastern Fertile Crescent. *Science* **353**, 499–503 (2016).

172. Brunel, S. et al. Ancient genomes from present-day France unveil 7,000 years of its demographic history. *Proc. Natl Acad. Sci. USA* **117**, 12791 (2020).

173. Cassidy, L. M. et al. Neolithic and Bronze Age migration to Ireland and establishment of the insular Atlantic genome. *Proc. Natl Acad. Sci. USA* **113**, 368–373 (2015).

174. Cassidy, L. M. et al. A dynastic elite in monumental Neolithic society. *Nature* **582**, 384–388 (2020).

Article

175. Damgaard, Pd. B. et al. 137 ancient human genomes from across the Eurasian steppes. *Nature* **557**, 369–374 (2018).
176. Damgaard, Pd. B. et al. The first horse herders and the impact of early Bronze Age steppe expansions into Asia. *Science* **360**, eaar7711 (2018).
177. Feldman, M. et al. Ancient DNA sheds light on the genetic origins of early Iron Age Philistines. *Sci. Adv.* **5**, eaax0061 (2019).
178. Fernandes, D. M. et al. The spread of steppe and Iranian-related ancestry in the islands of the western Mediterranean. *Nat. Ecol. Evol.* **4**, 334–345 (2020).
179. Fu, Q. et al. The genetic history of Ice Age Europe. *Nature* **534**, 200–205 (2016).
180. González-Fortes, G. et al. Paleogenomic evidence for multi-generational mixing between Neolithic farmers and mesolithic hunter-gatherers in the Lower Danube Basin. *Curr. Biol.* **27**, 1801–1810 (2017).
181. González-Fortes, G. et al. A western route of prehistoric human migration from Africa into the Iberian Peninsula. *Proc. R. Soc. B* **286**, 20182288 (2019).
182. Günther, T. et al. Population genomics of Mesolithic Scandinavia: investigating early postglacial migration routes and high-latitude adaptation. *PLoS Biol.* **16**, e2003703 (2018).
183. Haber, M. et al. Continuity and admixture in the last five millennia of Levantine history from Ancient Canaanite and present-day Lebanese genome sequences. *Am. J. Hum. Genet.* **101**, 274–282 (2017).
184. Harney, E. et al. Ancient DNA from Chalcolithic Israel reveals the role of population mixture in cultural transformation. *Nat. Commun.* **9**, 3336 (2018).
185. Hofmanová, Z. et al. Early farmers from across Europe directly descended from Neolithic Aegeans. *Proc. Natl Acad. Sci. USA* **113**, 6886–6891 (2016).
186. Järve, M. et al. Shifts in the genetic landscape of the Western Eurasian Steppe associated with the beginning and end of the Scythian dominance. *Curr. Biol.* **29**, 2430–2441 (2019).
187. Jones, E. R. et al. The Neolithic transition in the Baltic was not driven by admixture with early European farmers. *Curr. Biol.* **27**, 576–582 (2017).
188. Keller, A. et al. New insights into the Tyrolean Iceman's origin and phenotype as inferred by whole-genome sequencing. *Nat. Commun.* **3**, 698 (2012).
189. Krzewińska, M. et al. Ancient genomes suggest the eastern Pontic-Caspian steppe as the source of western Iron Age nomads. *Sci. Adv.* **4**, eaat4457 (2018).
190. Lamnidis, T. C. et al. Ancient Fennoscandian genomes reveal origin and spread of Siberian ancestry in Europe. *Nat. Commun.* **9**, 5018 (2018).
191. Lazaridis, I. et al. Ancient human genomes suggest three ancestral populations for present-day Europeans. *Nature* **513**, 409–413 (2014).
192. Lazaridis, I. et al. Genomic insights into the origin of farming in the ancient Near East. *Nature* **536**, 419–424 (2016).
193. Lazaridis, I. et al. Genetic origins of the Minoans and Mycenaeans. *Nature* **548**, 214–218 (2017).
194. Linderholm, A. et al. Corded Ware cultural complexity uncovered using genomic and isotopic analysis from south-eastern Poland. *Sci. Rep.* **10**, 6885 (2020).
195. Lipson, M. et al. Parallel palaeogenomic transects reveal complex genetic history of early European farmers. *Nature* **551**, 368–372 (2017).
196. Malmström, H. et al. The genomic ancestry of the Scandinavian Battle Axe Culture people and their relation to the broader Corded Ware horizon. *Proc. R. Soc. B* **286**, 20191528 (2019).
197. Marcus, J. H. et al. Genetic history from the Middle Neolithic to present on the Mediterranean island of Sardinia. *Nat. Commun.* **11**, 939 (2020).
198. Margaryan, A. et al. Population genomics of the Viking world. *Nature* **585**, 390–396 (2020).
199. Martiniano, R. et al. The population genomics of archaeological transition in west Iberia: investigation of ancient substructure using imputation and haplotype-based methods. *PLoS Genet.* **13**, e1006852 (2017).
200. Mathieson, I. et al. Genome-wide patterns of selection in 230 ancient Eurasians. *Nature* **528**, 499–503 (2015).
201. Mathieson, I. et al. The genomic history of southeastern Europe. *Nature* **555**, 197–203 (2018).
202. Mittnik, A. et al. Kinship-based social inequality in Bronze Age Europe. *Science* **93**, eaax6219 (2019).
203. Narasimhan, V. M. et al. The formation of human populations in South and Central Asia. *Science* **365**, eaat7487 (2019).
204. Olalde, I. et al. A common genetic origin for early farmers from Mediterranean Cardial and Central European LBK cultures. *Mol. Biol. Evol.* **32**, 3132–3142 (2015).
205. Olalde, I. et al. The Beaker phenomenon and the genomic transformation of northwest Europe. *Nature* **555**, 190–196 (2018).
206. Olalde, I. et al. The genomic history of the Iberian Peninsula over the past 8000 years. *Science* **363**, 1230–1234 (2019).
207. Rivollat, M. et al. Ancient genome-wide DNA from France highlights the complexity of interactions between Mesolithic hunter-gatherers and Neolithic farmers. *Sci. Adv.* **6**, eaaz5344 (2020).
208. Saag, L. et al. Extensive farming in Estonia started through a sex-biased migration from the Steppe. *Curr. Biol.* **27**, 2185–2193 (2017).
209. Sánchez-Quinto, F. et al. Megalithic tombs in western and northern Neolithic Europe were linked to a kindred society. *Proc. Natl Acad. Sci. USA* **116**, 9469–9474 (2019).
210. Schuenemann, V. J. et al. Ancient Egyptian mummy genomes suggest an increase of Sub-Saharan African ancestry in post-Roman periods. *Nat. Commun.* **8**, 15694 (2017).
211. Schroeder, H. et al. Unraveling ancestry, kinship, and violence in a Late Neolithic mass grave. *Proc. Natl Acad. Sci. USA* **116**, 10705–10710 (2019).
212. Skoglund, P. et al. Genomic diversity and admixture differs for Stone-Age Scandinavian foragers and farmers. *Science* **344**, 747–750 (2014).
213. Skourtanioti, E. et al. Genomic history of Neolithic to Bronze Age Anatolia, Northern Levant, and Southern Caucasus. *Cell* **181**, 1158–1175 (2020).
214. Unterländer, M. et al. Ancestry and demography and descendants of Iron Age nomads of the Eurasian Steppe. *Nat. Commun.* **8**, 14615 (2017).
215. Valdiosera, C. et al. Four millennia of Iberian biomolecular prehistory illustrate the impact of prehistoric migrations at the far end of Eurasia. *Proc. Natl Acad. Sci. USA* **115**, 3428–3433 (2018).
216. Villalba-Mouco, V. et al. Survival of Late Pleistocene hunter-gatherer ancestry in the Iberian Peninsula. *Curr. Biol.* **29**, 1169–1177 (2019).
217. Wang, C.-C. et al. Ancient human genome-wide data from a 3000-year interval in the Caucasus corresponds with eco-geographic regions. *Nat. Commun.* **10**, 590 (2019).
218. Allen Ancient DNA Resource (AADR): Downloadable genotypes of present-day and ancient DNA data. Version 44.3 https://reich.hms.harvard.edu/allen-ancient-dna-resource-aadr-downloadable-genotypes-present-day-and-ancient-dna-data (David Reich Lab, 2021).
219. Li, H. et al. The Sequence Alignment/Map format and SAMtools. *Bioinformatics* **25**, 2078–2079 (2009).
220. Felsenstein, J. *Theoretical Evolutionary Genetics* (Univ. of Washington, 2016).
221. Brest, J., Greiner, S., Boskovic, B., Mernik, M. & Zumer, V. Self-adapting control parameters in differential evolution: a comparative study on numerical benchmark problems. *IEEE Trans. Evol. Comput.* **10**, 646–657 (2006).
222. R Core Team. *R: A Language and Environment for Statistical Computing* (R Foundation for Statistical Computing, 2018).
223. Revell, L. J. learnPopGen: an R package for population genetic simulation and numerical analysis. *Ecol. Evol.* **9**, 7896–7902 (2019).
224. Jewett, E. M., Steinrücken, M. & Song, Y. S. The effects of population size histories on estimates of selection coefficients from time-series genetic data. *Mol. Biol. Evol.* **33**, 3002–3027 (2016).
225. Weninger, B., Joris, O. & Danzeglocke, U. CalPal-2007. *Cologne Radiocarbon Calibration & Palaeoclimate Research Package* (CalPal, 2007).
226. Galate, P. BANADORA, Banque de données des dates radiocarbones de Lyon pour l'Europe et le Proche-Orient http://www.archeometrie.mom.fr/banadora (Laboratoire ArAr, 2011).
227. Hinz, M. et al. RADON-Radiocarbon dates online 2012. Central European database of 14C dates for the Neolithic and the Early Bronze Age. *J. Neolit. Archaeol.* https://doi.org/10.12766/jna.2012.65 (2012).
228. Manning, K., Colledge, S., Crema, E. R., Shennan, S. & Timpson, A. The cultural evolution of Neolithic Europe. EUROEVOL Dataset 1: Sites, phases and radiocarbon data. *J. Open Archaeol. Data* **5**, e2 (2016).
229. Burrow, S. & Williams, S. *The Wales and Borders Radiocarbon Database* (Amgueddfa Cymru: National Museum Wales, 2008).
230. Ralston, I. & Ashmore, P. *Canmore Scottish Radiocarbon Database* https://canmore.org.uk/project/919374 (Historic Environment Scotland; accessed 14 July 2021).
231. Balsera, V., Díaz-del-Río, P., Gilman, A., Uriarte, A. & Vicent, J. M. Approaching the demography of late prehistoric Iberia through summed calibrated date probability distributions (7000–2000 cal BC). *Quat. Int.* **386**, 208–211 (2015).
232. Vermeersch, P. M. *Radiocarbon Palaeolithic Europe Database* v.18 (KU Leuven, 2015); https://ees.kuleuven.be/geography/projects/14c-palaeolithic/index.html
233. Bivand, R. & Lewin-Koh, N. maptools: Tools for handling spatial objects. R package version 1.1–2 (2021).
234. Brownrigg, R. mapdata: Extra map databases. R package version 2.3.0 (2018).
235. Hijmans, R. J. raster: Geographic data analysis and modeling. R package version 3.5–15 (2022).
236. Bivand, R. & Rundel, C. rgeos: Interface to geometry engine—open source ('GEOS'). R package version 0.5–9 (2021).
237. Neuwirth, E. RColorBrewer: ColorBrewer palettes. R package version 1.1–2 (2014).

Richard P. Evershed[1✉], **George Davey Smith**[2,3,4✉], **Mélanie Roffet-Salque**[1✉], **Adrian Timpson**[5,85], **Yoan Diekmann**[5,6], **Matthew S. Lyon**[2,3,4], **Lucy J. E. Cramp**[7], **Emmanuelle Casanova**[1], **Jessica Smyth**[1,8], **Helen L. Whelton**[1], **Julie Dunne**[1], **Veronika Brychova**[9,86], **Lucija Šoberl**[1], **Pascale Gerbault**[5,10], **Rosalind E. Gillis**[11,12], **Volker Heyd**[7,87], **Emily Johnson**[13,88], **Iain Kendall**[1], **Katie Manning**[14], **Arkadiusz Marciniak**[15], **Alan K. Outram**[13], **Jean-Denis Vigne**[11], **Stephen Shennan**[16], **Andrew Bevan**[16], **Sue Colledge**[16], **Lyndsay Allason-Jones**[17], **Luc Amkreutz**[18], **Alexandra Anders**[19], **Rose-Marie Arbogast**[20], **Adrian Bălăşescu**[21], **Eszter Bánffy**[22,23], **Alistair Barclay**[24], **Anja Behrens**[25], **Peter Bogucki**[26], **Ángel Carrancho Alonso**[27], **José Miguel Carretero**[28,29], **Nigel Cavanagh**[30], **Erich Claßen**[31], **Hipolito Collado Giraldo**[32,33], **Matthias Conrad**[34], **Piroska Csengeri**[35], **Lech Czerniak**[36], **Maciej Dębiec**[37], **Anthony Denaire**[38], **László Domborόczki**[39], **Christina Donald**[40], **Julia Ebert**[41], **Christopher Evans**[42], **Marta Francés-Negro**[28], **Detlef Gronenborn**[43], **Fabian Haack**[44], **Matthias Halle**[34], **Caroline Hamon**[45], **Roman Hülshoff**[46], **Michael Ilett**[45], **Eneko Iriarte**[28], **János Jakucs**[22], **Christian Jeunesse**[20], **Melanie Johnson**[47], **Andy M. Jones**[48], **Necmi Karul**[49], **Dmytro Kiosak**[50,51], **Nadezhda Kotova**[52], **Rüdiger Krause**[53], **Saskia Kretschmer**[34], **Marta Krüger**[54], **Philippe Lefranc**[55], **Olivia Lelong**[56,89], **Eva Lenneis**[57], **Andrey Logvin**[58], **Friedrich Lüth**[25], **Tibor Marton**[22], **Jane Marley**[59], **Richard Mortimer**[60], **Luiz Oosterbeek**[33,61,62], **Krisztián Oross**[22], **Juraj Pavúk**[63], **Joachim Pechtl**[64,90], **Pierre Pétrequin**[65], **Joshua Pollard**[66], **Richard Pollard**[67], **Dominic Powlesland**[68], **Joanna Pyzel**[36], **Pál Raczky**[19], **Andrew Richardson**[69], **Peter Rowe**[70,91], **Stephen Rowland**[71], **Ian Rowlandson**[72], **Thomas Saile**[73], **Katalin Sebők**[19], **Wolfram Schier**[41], **Germo Schmalfuß**[34], **Svetlana Sharapova**[74], **Helen Sharp**[67], **Alison Sheridan**[75], **Irina Shevnina**[58], **Iwona Sobkowiak-Tabaka**[76,92], **Peter Stadler**[57], **Harald Stäuble**[34], **Astrid Stobbe**[53], **Darko Stojanovski**[77,78], **Nenad Tasić**[79], **Ivo van Wijk**[80], **Ivana Vostrovská**[81,93], **Jasna Vuković**[79], **Sabine Wolfram**[82], **Andrea Zeeb-Lanz**[83] & **Mark G. Thomas**[5,84✉]

[1]Organic Geochemistry Unit, School of Chemistry, University of Bristol, Bristol, UK. [2]MRC Integrative Epidemiology Unit, University of Bristol, Bristol, UK. [3]Population Health Sciences, Bristol Medical School, University of Bristol, Bristol, UK. [4]NIHR Bristol Biomedical Research Centre, University of Bristol, Bristol, UK. [5]Department of Genetics, Evolution and Environment, University College London, London, UK. [6]Palaeogenetics Group, Institute of Organismic and Molecular Evolution (iomE), Johannes Gutenberg University Mainz, Mainz, Germany. [7]Department of Anthropology and Archaeology, University of Bristol, Bristol, UK. [8]School of Archaeology, University College Dublin, Dublin, Ireland. [9]Department of Dairy, Fat and Cosmetics, University of Chemistry and Technology Prague, Prague, Czech Republic. [10]School of Life Sciences, University of Westminster, London, UK. [11]Archéozoologie, Archéobotanique: Sociétés, Pratiques et Environnement (UMR 7209), CNRS–Muséum National d'Histoire Naturelle–Sorbonne Universités, Paris, France. [12]ICArEHB, Faculdade de Ciências Humanas e Sociais, Universidade do Algarve, Faro, Portugal. [13]Department of Archaeology, University of Exeter, Exeter, UK. [14]Department of Geography, King's College London, London, UK. [15]Institute of Prehistory, Adam Mickiewicz University, Poznań, Poland. [16]UCL Institute of Archaeology, University College London, London, UK. [17]Great North Museum (former Museum of Antiquities), Newcastle, UK. [18]National Museum of Antiquities, Leiden, the Netherlands. [19]Institute of Archaeological Sciences, Eötvös Loránd University, Budapest, Hungary. [20]UMR 7044, ARCHIMEDE, University of Strasbourg, Strasbourg, France. [21]Department of Bioarchaeology, 'Vasile Pârvan' Institute of Archaeology, Romanian Academy, Bucharest, Romania. [22]Institute of Archaeology, Research Centre for the Humanities, Eötvös Loránd Research Network, Centre of Excellence of the Hungarian Academy of Sciences, Budapest, Hungary. [23]Römisch-Germanische Kommission, Frankfurt, Germany. [24]Cotswold Archaeology, Cirencester, UK. [25]German Archaeological Institute, Berlin, Germany. [26]School of Engineering and Applied Science, Princeton University, Princeton, NJ, USA. [27]Área de Prehistoria, Departamento de Historia, Geografía y Comunicación, University of Burgos, Burgos, Spain. [28]Laboratorio Evolución Humana, University of Burgos, Burgos, Spain. [29]Centro Mixto UCM-ISCIII de Evolución y Comportamiento Humana, Madrid, Spain. [30]Network Archaeology, Lincoln, UK. [31]LVR-State Service for Archaeological Heritage, Bonn, Germany. [32]Patrimonio & Arte Research Group, Extremadura University, Badajoz and Cáceres, Badajoz, Spain. [33]Geosciences Centre, Coimbra University, Coimbra, Portugal. [34]Landesamt für Archäologie, Dresden, Germany. [35]Herman Ottó Museum, Miskolc, Hungary. [36]Institute of Archaeology and Ethnology, University of Gdańsk, Gdańsk, Poland. [37]Institute of Archaeology, University Rzeszów, Rzeszów, Poland. [38]UMR 6298, ARTEHIS, University of Burgundy, Dijon, France. [39]Dobó István Castle Museum, Eger, Hungary. [40]The McManus: Dundee's Art Gallery & Museum, Dundee, UK. [41]Institute of Prehistoric Archaeology, Free University of Berlin, Berlin, Germany. [42]Cambridge Archaeological Unit, University of Cambridge, Cambridge, UK. [43]Römisch-Germanisches Zentralmuseum, Leibniz Research Institute for Archaeology, Mainz, Germany. [44]Archaeological Department, Landesmuseum Württemberg, Stuttgart, Germany. [45]UMR 8215, Trajectoires, Université Paris 1 Panthéon-Sorbonne, Paris, France. [46]State Office for Heritage Management and Archaeology, Saxony Anhalt/State Museum of Prehistory, Halle/Saale, Germany. [47]CFA Archaeology, Musselburgh, UK. [48]Cornwall Archaeological Unit, Cornwall Council, Truro, UK. [49]Istanbul University, Istanbul, Turkey. [50]'I.I. Mechnikov', Odessa National University, Odessa, Ukraine. [51]Ca' Foscari, University of Venice, Venice, Italy. [52]Institute of Archaeology of Academy of Science of Ukraine, Kiev, Ukraine. [53]Prehistory Department, Institut of Archaeology, Johann Wolfgang Goethe-Universität, Frankfurt, Germany. [54]Department of Archaeology, Adam Mickiewicz University, Poznań, Poland. [55]UMR 7044, INRAP Grand-Est Sud, University of Strasbourg, Strasbourg, France. [56]GUARD Glasgow, Glasgow, UK. [57]Department of Prehistoric and Historical Archaeology, University of Vienna, Vienna, Austria. [58]Kostanay State University, Kostanay, Kazakhstan. [59]Royal Cornwall Museum, Truro, UK. [60]Oxford Archaeology East, Oxford, UK. [61]Polytechnic Institute of Tomar, Tomar, Portugal. [62]Terra e Memória Institute, Mação, Portugal. [63]Archeologický ústav SAV, Nitra, Slovakia. [64]Kelten Römer Museum Manching, Manching, Germany. [65]MSHE C.N. Ledoux, CNRS & University of Franche-Comté, Besançon, France. [66]Department of Archaeology, University of Southampton, Southampton, UK. [67]Leicestershire County Council Museums, Leicestershire, UK. [68]The Landscape Research Centre Ltd., West Heslerton, UK. [69]Canterbury Archaeological Trust, Canterbury, UK. [70]Tees Archaeology, Hartlepool, UK. [71]Oxford Archaeology North, Lancaster, UK. [72]Archaeological Consultancy, Emsworth, UK. [73]Institute of History, University of Regensburg, Regensburg, Germany. [74]Institute of History and Archaeology, UB RAS, Ekaterinburg, Russia. [75]National Museums Scotland, Edinburgh, UK. [76]Institute of Archaeology and Ethnology, Polish Academy of Sciences, Poznań, Poland. [77]Geology Department, University of Trás-os-Montes and Alto Douro, Vila Real, Portugal. [78]Department of Humanistic Studies, University of Ferrara, Ferrara, Italy. [79]University of Belgrade, Belgrad, Serbia. [80]Faculty of Archaeology, Leiden University, Leiden, the Netherlands. [81]Institute of Archaeology and Museology, Masaryk University, Brno, Czech Republic. [82]Staatliches Museum für Archäologie, Chemnitz, Germany. [83]Generaldirektion Kulturelles Erbe Rheinland-Pfalz, Dir. Landesarchäologie, Speyer, Germany. [84]UCL Genetics Institute, University College London, London, UK. [85]Present address: Max Planck Institute for the Science of Human History, Jena, Germany. [86]Present address: Nuclear Dosimetry Department, Institute of Nuclear Physics of the Czech Academy of Sciences, Prague, Czech Republic. [87]Present address: Department of Cultures, Section of Archaeology, University of Helsinki, Helsinki, Finland. [88]Present address: Archaeology South-East, UCL Institute of Archaeology, University College London, London, UK. [89]Present address: Eunomia Research & Consulting, Bristol, UK. [90]Present address: Department of Archaeology, University of Innsbruck, Innsbruck, Austria. [91]Present address: North Yorkshire County Council HER, Northallerton, UK. [92]Present address: Faculty of Archaeology, Adam Mickiewicz University, Poznań, Poland. [93]Present address: Department of History, Palacký University, Olomouc, Czech Republic. [✉]e-mail: R.P.Evershed@bristol.ac.uk; KZ.Davey-Smith@bristol.ac.uk; melanie.salque@bristol.ac.uk; m.thomas@ucl.ac.uk

Article

Methods

Lipid residue analyses

Data, lipid extraction and analysis. Our lipid residue analysis draws on our SQL database of 13,181 archaeological potsherds from 554 sites, of which 6,899 sherds have yielded animal fat residues from georeferenced sites and dated phases (826 phases from 554 sites). This analysis represents about 30% new data (Supplementary Table 1) and about 70% collated from previously published studies[3,11,12,15–18,20–22,33,84–159].

Lipid residue analyses and interpretations were based on established protocols[160,161]. Lipids were extracted from 1–3 g of cleaned potsherd and analysed using gas chromatography (GC) and GC–mass spectrometry (GC–MS) to determine their molecular composition. Compound-specific $\delta^{13}C$ values of fatty acids were determined using Agilent Industries 7890A gas chromatograph coupled to an Isoprime 100 isotope ratio mass spectrometer (GC-C-IRMS) for extracts identified as animal fats. Samples were introduced via a split/splitless injector in splitless mode onto a 50 m × 0.32 mm fused silica capillary column coated with a HP-1 stationary phase (100% dimethylpolysiloxane, Agilent, 0.17 µm). The GC oven temperature programme was set to hold at 40 °C for 2 min, followed by a gradient increase to 300 °C at 10 °C min^{-1}; the oven was then run isothermally for 10 min. Helium was used as a carrier gas and maintained at a constant flow of 2 ml min^{-1}. The combustion reactor consisted of a quartz tube filled with copper oxide pellets which was maintained at a temperature of 850 °C. Each sample was run at least in duplicate. Instrument stability was monitored by running a fatty acid methyl ester standard mixture every two or four runs. The $\delta^{13}C$ values are the ratios $^{13}C/^{12}C$ and expressed relative to the Vienna Pee Dee Belemnite, calibrated against a CO_2 reference gas injected directly in the ion source as two pulses at the beginning of each run. Instrumental precision was 0.3‰. Data processing was carried out using Ion Vantage software (v.1.5.6.0, IsoPrime).

$\Delta^{13}C$ proxy for milk exploitation. The $\delta^{13}C$ values of the $C_{16:0}$ and $C_{18:0}$ fatty acids from more than 170 modern ruminant adipose and dairy fats taken from animals raised in Europe, Eurasia and Africa, reveal a consistent difference in the $\delta^{13}C$ values of the $C_{18:0}$ fatty acid, which relate to the different biosynthetic origins of this fatty acid in the two fat types[16,47]. The result is that $\delta^{13}C$ values of the $C_{18:0}$ fatty acid in milk are always depleted compared to the $C_{18:0}$ fatty acid in ruminant adipose fats by on average 2.3‰ (ref. [16]). This difference allows archaeological ruminant fats extracted from pottery to be assigned as either milk or adipose fats. Initial reference fats were taken from animals grazing in a pure C_3 plant-dominated pasture in the UK and archaeological investigations of dairying in historically pure C_3 regions can be achieved by comparisons with the raw $\delta^{13}C$ values, for example, refs. [16,47]. However, in regions where C_4 plants are present and other environmental factors (for example, high aridity) affect the raw $\delta^{13}C$ values, the $\Delta^{13}C$ values ($\Delta^{13}C = \delta^{13}C_{18:0} - \delta^{13}C_{16:0}$) are used to remove the environmental effects (for example, refs. [2,48]). For modern reference fats, ruminant milk fats are distinguished from ruminant adipose fats in displaying $\Delta^{13}C$ values ≤−3.1‰, ruminant adipose fats between −3.1 and −0.3‰, with non-ruminant fats at >−0.3‰. Individual archaeological pottery lipid extracts are assigned to fat type on the basis of their $\Delta^{13}C$ values using the ranges defined by the reference fats.

Animal fats extracted from potsherds are categorized as containing milk lipids if their $\Delta^{13}C$ ($= \delta^{13}C_{18:0} - \delta^{13}C_{16:0}$) values are below the threshold −3.1‰ or non-milk otherwise[48]. Although this threshold choice influences the absolute proportion estimates, it has almost no influence when evaluating the fluctuations in milk use through time, as the relative proportions will be largely unaffected (Supplementary Fig. 1). Indeed, even if the exact number of sherds containing dairy fat residues were known, this could not be used as a proxy for milk proportion in overall diets because of biases in pottery use. Similarly, our conclusion that milk exploitation was widespread throughout the Neolithic period is also based on the observation that the proportion of sherds with dairy fat residues were similar to that of the Bronze Age.

Chronology. Archaeological sherds are associated in the MySQL database with specific site phases. Each phase is assigned a uniform date range using published start and end dates from archaeological site reports. If unavailable, we used calibrated[162] radiocarbon dates to construct phase models in OxCal[163] and used the mode of each boundary posterior distribution as start and end dates. In cases in which neither of these sources was available (10% of phases), phases 'borrow' their chronology from the geographically closest site phase that has the same associated culture. Date ranges of site phases are reasonably constrained (75% less than 580 years).

UK Biobank analysis

Data. UK Biobank[4,5] is a large prospective cohort study of approximately 500,000 UK participants aged 37–73 years at recruitment (2006–2010). The study collected a wide-range of measures including demographics, health status, lifestyle, cognitive function, mental and physical health and molecular data such as genetic and biomarkers. UK Biobank received ethical approval from the Research Ethics Committee (REC reference for UK Biobank is 11/NW/0382). All analyses were performed under application no. 16729.

Dairy consumption. Multiple measures of milk consumption were evaluated in this study.
Milk servings. Participants were asked: How many glasses/cartons/250 ml of milk (excluding milkshakes) did you consume yesterday? (field 100520) and how many glasses/cartons/250 ml of yogurt drinks, flavoured milk or milkshakes did you consume yesterday? (field 100530). These measures were only asked if participants drank some milk the previous day and therefore there was no zero servings value. To reduce missingness, mean servings were calculated from five repeated measures taken in 2009–2012.
Dairy milk preference. Participants were asked at baseline: What type of milk do you mainly use? (field 1418). From this variable binary non-dairy versus dairy consumption was derived: soya and never/rarely have milk versus full cream, semi-skimmed and skimmed.
Lactose-free diet. Participants were asked: Do you routinely follow a special diet? Respondents answering 'Yes' to diet for lactose intolerance on any of the five repeated measures undertaken during 2009–2012 were compared against participants answering 'No' to all non-missing responses.

Genetic data. We focused on the major European LP variant located upstream of the coding gene promotor (rs4988235-A, LCT-13,910*T) (ref. [30]). The lactase genotype showed strong departure from Hardy–Weinberg equilibrium (HWE) in UK Biobank white British participants (Extended Data Table 2; $\chi^2 = 76.93$; $P = 1.80 \times 10^{-18}$) using the Hardy–Weinberg R package (v.1.6.3) (ref. [164]). This finding could arise from non-random mating, ascertainment bias, genotyping error or population stratification/admixture[52]. The last was mitigated as far as reasonably possible using a homogenous population which was clearly effective when considering the more extreme HWE violation in 'any other white background' group (Extended Data Table 2; $\chi^2 = 423.57$; $P = 4.10 \times 10^{-94}$). HWE violation was also observed in gnomAD[165] which contains genotype frequencies on 33,992 non-Finnish Europeans using whole genome sequencing (Extended Data Table 2; $\chi^2 = 300.32$; $P = 2.81 \times 10^{-67}$). Sequencing and array technologies have distinct error profiles and therefore technical artefact is an unlikely explanation.

Crude gene association with consumption. Unadjusted genotype frequencies stratified by dairy consumption were calculated from an unrelated white British subsample of UK Biobank prepared according to ref. [166].

Gene association with health outcomes. Variant association with health outcomes was performed using an unrelated white British

subset of UK Biobank for the main analysis and within-family estimates for sensitivity analyses. Time-to-death was estimated using a Cox proportional hazards model. All-cause mortality was derived from field date-of-death (40000). The following fields within the UK Biobank were used: body mass index (21001); father's age at death (1807); heel bone mineral density (78); IGF-1 (30770); mother's age at death (3526); number of children fathered (2405); number of live births (2734); standing height (50); vitamin D (30890). All models assumed additive inheritance and were adjusted for age, sex and top 40 genetic principal components. Within-family estimates were produced as previously described for continuous[167] and binary outcomes[168]. Date-of-death was obtained from linkage with death registries. All other outcomes were collected at baseline.

Assortative mating influence on lactase persistence. To determine whether milk consumption influences mate choice and therefore invalidates HWE assumptions[52], we estimated the spousal LP genetic correlation (Extended Data Table 3) adjusted for age, the top ten genetic principal components, partner age and partner top ten genetic principal components. Under an additive linear model there was very weak evidence in support of assortative mating on LP (0.004 mean increase in partner LP allele per increase in individual LP allele (95% CI −0.002, 0.011)). However, a single allelic copy of LP is sufficient to produce the observable phenotype of lactase persistence (which produces a very small influence on milk intake; Table 1) and therefore we considered a dominant inheritance model (imputed variant dosage capped at one; rs4988235 GG versus GA and AA). We term individuals with GA or AA 'lactase persistent'. Using logistic regression, we found that lactase persistent individuals were at 10% increased odds of selecting a lactase persistent partner (1.10 odds ratio (OR) (95% CI 1.00, 1.22) for partner being lactase persistent). The effect was consistent under sensitivity conditions additionally adjusting for the top 40 genetic principal components (mean increase of 1.11 OR (95% CI 1.00, 1.22) partner having one or more copies of LP among LP individuals) reducing the possibility that partner selection was driven entirely by population stratification.

Spousal pairs were derived and validated in a European subsample of UK Biobank ($n = 47,459$) supplied by L. Howe, MRC IEU[51]. Analyses were restricted to spousal pairs with complete data ($n = 46,560$).

Ancient DNA analyses
Data. We collated published BAM files from 2,999 ancient Eurasian individuals[25,27,169–217], out of which 1,786 had the European LP single nucleotide polymorphism (SNP) covered at least once (read depth: span 1 to 128-fold, average sevenfold). All genomes came aligned to the GRCh37/hg19 human reference assembly but for the Tyrolean Iceman (hg18). Relevant geographic and temporal annotation was extracted from D. Reich's aDNA compendium v.44.3 (ref. [218]), see Fig. 3 for a representation of the full dataset. For the joint analyses of genetic and ecological data, we restricted this dataset to those individuals spatiotemporally overlapping the ecological data (four geographic regions: 'British Isles', 'Rhine−Danube axis', 'Mediterranean Europe' and the 'Baltic region'; 8,000–2,500 years BP), leaving 2,162, out of which 1,293 had the lactase locus covered at least once (read depth: span 1–128-fold, average sevenfold).

We extracted the pileup at the position of the European LP SNP (rs4988235; in hg19, chromosome 2, position 136608646; hg18, chromosome 2, position 136325116) with default quality cut-offs using Samtools[219]. For sites with read depth at least two, we called the diploid genotype with the highest likelihood; for sites covered only once, only a single allele was called. Exceptions are individuals PEN001_real2 (ref. [207]) and Klei10 (ref. [185]), which each have one out of four reads with the derived allele. However, as discussed in the respective publications, the ages of the samples suggest that the derived alleles are rather the consequence of post-mortem damage and we therefore consider both of them as homozygous ancestral.

Likelihood comparison of selection drivers. Many phenomena have the potential to influence LP allele frequency trajectories in each of our geographic regions, including selection, migration, genetic drift and population structure. We explore just one of these factors in isolation−selection−to test if the observed archaeological allele frequencies are best explained purely under a null model of constant selection or might be partly explained by a model whereby the intensity of selection varies through time in accordance with a suggested ecological driver. Although selection strength cannot be observed directly, population genetic models describe its effect on expected allele frequencies. Given the set of ecological proxy variables that we suggest may act as selective agents, we can ask if fluctuating selection models based on these variables fit the genetic data better than a null model of constant selection strength. If a fluctuating model fits best, we may infer that the ecological proxy is linked to the true selective agent.

We obtain a likelihood equation in the following way. Say $m(t)$ is a time series over time t, with $m(t) \in [0, 1]$. We describe its effect on selection strength s as $s(t) = b \times m(t)^{\frac{1}{a}-1}$, in which $b \in [0, 1]$ is the maximal selection coefficient modulated by a factor that depends on the time series and an exponent $a \in]0, 1]$. Note that with $a = 1$ the model simplifies to one of constant selection strength b.

As selection on lactase is strong, we assume a deterministic allele frequency trajectory, ignoring random drift. We assume a generation time of 28 years. In case of an additive model for selection−corresponding to relative fitnesses $1 + 2s$, $1 + s$ and 1 for homozygous derived, heterozygous and homozygous ancestral genotypes, respectively−we approximate the expected allele frequency after t generations (divide by generation time to scale to years) by $\frac{y_0}{y_0 + (1-y_0)e^{-st}}$, with an additional model parameter y_0 for the initial allele frequency at time point t_0 (here set at 8,000 years BP). This avoids the challenges of estimating the date of the LP mutation by assuming it was present in the population at t_0 at some unknown frequency, y_0. Moreover, this avoids modelling the lowest frequency part of the allele trajectory for which drift is strongest.

In most cases, $m(t)$ will be piecewise constant over time windows of the order of a hundred years, meaning that $s(t)$ is piecewise constant as well and allele frequencies can be computed in between these boundaries with the equation above setting the initial frequency of later time intervals to the last one of the preceding time interval.

The dominant model−corresponding to relative fitnesses $1 + s, 1 + s$ and 1 for homozygous derived, heterozygous and homozygous ancestral genotypes, respectively−is considered here as well, as the LP phenotype has been shown to be dominant. It requires numerical optimization of an approximation, as no exact expression for $y(t)$ as a function of y_0, s and t exists. The value $y(t)$ can be obtained by keeping y_0, s and t constant and adjusting $y(t)$ until equation $t = \frac{1}{s}\left[-\frac{1}{1-y_0} + \ln\left(\frac{1-y_0}{y_0}\right) + \frac{1}{1-y_t} - \ln\left(\frac{1-y_t}{y_t}\right) - s\ln\left(\frac{y_0}{y_t}\right) \right]$ is satisfied[220]. As above, this allows us to compute expected deterministic allele frequency trajectories for piecewise constant selection strengths. Note that owing to the parameterization of fitness, the dominant selection coefficient has to be multiplied by a factor 2 to be comparable to the additive model.

For an expected allele frequency trajectory over the entire time range under one of the above inheritance models, the log likelihood given k observed ancestral alleles at time points t_i and n derived alleles observed at time points t_j is computed as $\sum_{i=1}^{k} \ln(1 - y(t_i)) + \sum_{j=1}^{n} \ln y(t_j)$. We were able to construct ecological proxy variables for four distinct regions, with different time series $m(t)$ and therefore different expected allele frequency trajectories. To analyse these regions jointly, log likelihoods were summed over all four regions, to result in a single optimal parameter combination across all regions.

Article

For a given time series $m(t)$ we optimized the model parameters y_0 (initial allele frequency at time point 0), a and b (with $a = 1$ fixed for the constant selection strength model) using the 'JDEoptim' function from the 'DEoptimR' library[221] in R (ref. [222]). We chose the best parameter combination from six independent runs, three with and three without initializing JDEoptim with the parameters found for the constant selection model.

Finally, statistical model comparison was performed by computing P values obtained from a likelihood ratio test accounting for the different number of parameters between constant and fluctuating models (two and three, respectively). We controlled the false discovery rate in the multiple testing of different models with the Benjamini–Hochberg procedure, ordering the P values, $P_1 \leq P_2 \leq \ldots \leq P_m$ and declare a test of rank j non-significant at level δ if $P_j > \delta \frac{j}{m}$.

Power analysis. We analysed the power of our approach to estimate parameters and detect ecological proxies linked to selection strength via simulations. We chose to focus on milk exploitation, in particular to assess the robustness of our finding that milk is unlikely to drive selection on the LP allele.

First, we simulated genotypes under nine different model parameter combinations, with three replicates per combination, sampling a matching number of alleles (one or two) at the corresponding time points in the real data. Supplementary Fig. 2 shows the results for all combinations of $s \in \{0.02, 0.035, 0.05\}$ and $a \in \{0.2, 0.6, 0.8\}$, with an initial frequency y_0 fixed at 0.005. We observe that both parameters can be estimated accurately when $s > 0.02$ or $a > 0.25$. Models with small values for s or a are most challenging as both lead to small selection coefficients on average (small values for a lead to very few bursts of high selection over a background of otherwise weak selection; for example, Extended Data Fig. 4) and, therefore, a generally low number of sampled derived alleles. Supplementary Fig. 3 illustrates this phenomenon, in which absolute errors in the estimates of s and a for three replicate simulations per parameter combination above repeated independently for three different initial frequencies $y_0 \in \{0.0005, 0.005, 0.01\}$, are plotted against the number of simulated derived alleles. High estimation errors are exclusively found when few derived alleles are simulated, as the latter are responsible for important likelihood differences between models with appreciable LP allele frequencies. The number of derived alleles in our dataset seems to be high enough to estimate s with high accuracy and a at least with intermediate accuracy. Besides the estimation of actual model parameters, we quantified the power to select a model with milk as a driver over a constant selection model. For the same set of simulations underlying Supplementary Fig. 3, we show the likelihood differences between a model of constant selection and one in which milk exploitation drives selection strength on the derived LP allele in Supplementary Fig. 4. With less than 30 derived alleles, which is the number we observe in the actual data, only 20% of the likelihood differences pass the significance threshold, compared to 81% for simulations with at least the same number of derived alleles (51% overall), in which we restricted the set of simulations only to those with an estimated parameter a above 0.95 (values close to one effectively lead to constant selection models and therefore a likelihood difference close to zero). We are therefore confident that, if milk acted as a driver of selection strength in our data, we would at least find a meaningfully increased likelihood.

Second, we assessed the impact of noise in the ecological proxies, here exemplarily and most importantly in the context of this study on milk exploitation. To simulate inaccuracies, we multiplied each constant piece of the milk exploitation proxy by a random number uniformly drawn from the interval [0.5, 1.5], leading to a 'noisy' version that differs from the original values on average by 0.091 (corresponding to about 11% of the milk variable's full range from 0 to about 0.8; maximum deviation 0.32). Supplementary Fig. 5 compares parameter estimates and likelihoods with the values found in the corresponding simulation shown in Supplementary Fig. 2. Although there are outliers with noticeable deviation when $a = 0.25$ (most challenging to distinguish from a constant selection model as discussed above), the remaining parameter estimates are barely affected and none of the likelihoods change across the significance threshold. Therefore, we consider our approach robust against moderate levels of noise in the milk exploitation proxy and more generally in other time series.

Lastly, we sought to quantify the effect that drift—which we are not explicitly modelling—may have on our inferences. We repeated the experiments shown in Supplementary Figs. 2–4, however, simulating allele frequency trajectories with fluctuating selection and drift as the basis from which alleles are drawn with the sampling strategy described above that emulates our real aDNA data (drift simulations only with initial frequency $y_0 = 0.005$). We used the 'learnPopGen' R library[223] and simulated two levels of drift by setting the effective population size to $N_e \in \{1,000, 10,000\}$ (generation time implemented by extending allele frequencies per generation to piecewise constant frequencies lasting 28 years). We observe that the ability to accurately infer s is only mildly affected, whereas the effect on a is stronger (Supplementary Fig. 6). This is in line, for example, with ref. [224] in which the authors find limited benefit to explicitly model drift for the inference of selection coefficients. Plotting the same data differently shows that the relationship with the number of simulated derived alleles continues to hold, although the accuracy of a estimates drops with stronger drift even at high numbers of simulated derived alleles (Supplementary Fig. 7). Importantly, the ability to detect significant likelihood differences in the presence of drift is not affected (Supplementary Fig. 8), as detailed in Extended Data Table 4. Hence, we consider our modelling to be robust against mild levels of drift and a deterministic model to be appropriate, especially as selection coefficients are known to have been high on the derived LP allele and as our geographic regions are large enough to warrant high effective population sizes.

In conclusion, our approach performs well at estimating parameters, especially when the number of derived alleles is at least that in the real aDNA data we curated for this paper and, most importantly, has the power to select a fluctuating selection model over a constant selection model, even in the presence of moderate drift and noise in ecological driver variables.

Ecological proxy variables

We generate five ecological variables as proxies for suggested drivers of LP selection. Each variable is generated for four geographic polygons which overlap spatially and temporally with our ancient genetic data ('British Isles', 'Baltic region', 'Rhine–Danube axis' and 'Mediterranean Europe'). We make no assumption about the direction of the possible relationship between each variable (V) and the selection coefficient (that is, if they are positively or negatively correlated). Therefore, we also generate a set of inverse variables, which can be notionally considered as a reflection; for example, a variable that ranges between 0 and 1 will have an inverse variable between 1 and 0.

Radiocarbon dates. Two of the five ecological variables (residential density and fluctuations in population levels) were constructed directly by using an extensive database comprising >110,000 ^{14}C dates which we compiled from over 1,000 published sources including CalPal[225], BANADORA[226], RADON[227], EUROEVOL[228], Wales and Borders radiocarbon database[229], Scottish Radiocarbon Database[230], ref. [231] and the Palaeolithic Europe Database[232], which provided most radiocarbon dates. A summary of the radiocarbon dates used within our four polygons can be found at https://github.com/AdrianTimpson/2020-03-03523A and a full list of sources is available on request.

Residential density (clustering). Under the assumption that dwelling proximity increases the potential for the spread of disease in a

population, our 'chronic' mechanism proposes that periods and regions of greater residential density would tend to suffer more from diseases, providing greater selection on LP. We construct a residential density statistic (RDS) from the site locations of our radiocarbon database. The RDS is influenced neither by the number of archaeological sites (which is heavily biased by differential sampling and a general increase through the Neolithic period from population growth) nor by geographic structure in the site locations (caused by features such as islands and mountains). Instead, our RDS uses the distribution of pairwise distances between all sites in a region as a null expectation and then calculates how the distribution of pairwise distances in each time slice deviates from this expected distribution. We achieve this by first generating the empirical cumulative distribution function (ECDF) of pairwise distances of all sites ($ECDF_{all}$), then for a single time slice we generate the ECDF of pairwise distances of sites that fall within that time slice ($ECDF_t$). We then calculate the RDS in that slice as $sum(ECDF_t - ECDF_{all})$. This is repeated for each time slice, giving a vector of RDS values. Given that there is substantial chronological uncertainty for each site, we also use associated radiocarbon dates to generate a summed probability distribution (SPD) after calibrating through IntCal13 (ref. [162]). We use the 99% quantiles of this SPD as a conservatively wide date range for the site. We then uniformly sample a date from this range, to assign each site to just one time slice. The entire process is repeated 500 times to generate 500 RDS vectors. This allows CIs to be generated that incorporate the chronological uncertainty in the dataset and we use the mean of these 500 replicates as the final time series in the LP model.

Animal exploitation. Fluctuations between domestic and wild animal exploitation for meat have the potential to inform on various economic, social and food production changes. For example, we might expect an increase in the proportion of domesticates to be associated with greater animal husbandry and increased contact with animals could lead to a greater probability of zoonotic diseases and therefore greater selection. Conversely, we might expect periods of famine from failure of agriculture to result in a return to exploiting wild resources, thus a decrease in domestic animals might correlate with periods (and regions) with greater selection. We extract NISP counts of the main meat-bearing taxa for domestic (*Bos taurus*, *Sus scrofa domesticus*, *Ovis aries*, *Capra hircus*, *Equus caballus*) and wild (*Bos primigenius*, *Sus scrofa scrofa*, *Cervus elaphus*, *Alces alces*, *Rupicapra rupicapra*, Cervidae, *Oryctolagus cuniculus*, *Lepus europaeus*, Lagomorpha, *Equus ferus*) from the EUROEVOL[71] and OSSK[49] databases. Therefore, for a given time slice the 'domesticates' and 'wild' NISP counts are used to calculate a proportion of domesticates.

Fluctuations in population levels. We use our radiocarbon database and the R package ADMUR to directly model the underlying broadscale population dynamics as the combination of exponential population growth with power law taphonomic loss. An SPD was also generated and the residual difference between the short-term fluctuations of the SPD and the long-term trend of the model was used as the detrended proxy for short-term fluctuations in human presence through time. This was achieved independently for each of the four geographic polygons, after all radiocarbon dates were calibrated through the intcal20 curve[162] Finally, we normalize these residuals to a range between 0 and 1 globally, by scaling each variable by the smallest and largest values found across all polygons. In all cases, to adjust for ascertainment bias, radiocarbon dates in a site phase were first aggregated and normalized, so that the total probability mass for each site phase was 1, no matter how many radiocarbon dates at a site phase.

Solar insolation. We calculate mean annual solar insolation at 0.5 × 0.5 degree resolution using modern data (1983 to 2013) from NASA's midday insolation incident on a horizontal surface[81] (W m^{-2}).

Values at each grid point are then used to calculate a single mean value for each of the four geographic polygons. Therefore, unlike the previous ecological variables that each comprise three time series, solar insolation (and its inverse) are not time variable. No doubt insolation would have fluctuated over the study period but the magnitude of this variation is trivial compared to the variation between polygons. These values are then normalized to a range between 0 and 1 by dividing by the Earth's single greatest mean annual solar insolation value of 867.90 W m^{-2}.

Time-series plots and interpolation maps

We account for three sources of uncertainty when estimating frequencies from count data (LP and LNP alleles, potsherds with and without dairy fat residues, domestic and wild species NISP). Within any time slice we have multiple site phases, each of which has integer counts of presence and absence. Sample sizes vary hugely between site phases (potsherds between 1 and 121, NISP between 1 and 61,497) and our objective is to fairly estimate the 'underlying' frequencies of these count data across all these site phases. We ensure that each site contributes fairly to this estimate, by weighting by the precision of each site's frequency estimate (a function of sample size n, for which the weight is defined by $1 - 1/\sqrt{(n+1)}$).

In addition, to fairly incorporate in our estimate the uncertainty both from small sample size and chronology, we adopt a three-stage sampling process in our estimate, which is repeated 5,000 times to also find the maximum a posteriori and confidence interval. The first stage randomly samples a single frequency from a Beta distribution, in which the two shape parameters are the observed presence and absence counts in the site phase. This includes an additional one count of each as a uniform prior. The second stage randomly samples a date from the site phase's date range. This then allows us to assign each phase to exactly one time slice. The third stage then calculates the weighted average frequency of the site phases (in each time slice), weighted according to their sample size as explained above. Where a phase spans two (or more) time slices, its contribution to each slice is weighted accordingly.

Interpolated maps of the frequency of dairy fat residues (Fig. 2) were achieved with a new kernel density approach that generates both the interpolated frequencies using colour hue and confidence in the interpolation using colour saturation. The interpolated surface was masked to coastlines and used the following R libraries: maptools[233], mapdata (original S code by R. A. Becker and A. R. Wilks; R version by ref. [234]), raster[235], rgeos[236] and RColorBrewer[237]. We constructed a two-dimensional Gaussian kernel for each site phase, the magnitude of which was weighted by the precision of the estimate, using $1 - 1/\sqrt{(n+1)}$ for which n is the number of sherds that have yielded animal fats. The frequency of dairy residues at any geographic point was then calculated as the average of the proportion of sherds containing dairy fat residues over the total number of sherds yielding residues at a given site phase, weighted by the probability density function of each site phase's kernel at that point. Therefore, the influence each site phase has on any interpolated point on the map depends primarily on its geographic distance from that point but is also influenced by the error on its frequency estimate. This second influence is small in comparison because the most extreme difference in the relative contribution of sites is only threefold (0.909 for which $n = 121$ compared to 0.293 for which $n = 1$). The combined surface of two-dimensional Gaussian kernels (for all site phases) generated during the interpolation then determines the colour saturation, to illustrate geographic regions where there is an absence of data. Conceptually this approach describes the idealized process of shooting paintballs at a grey map. A paintball corresponds to the information content at a site phase, such that its central position is determined by the site's latitude and longitude; hue is determined by the dairy fat frequency; and size of paintball is determined by the precision.

Article

Two further parameters are required. Firstly, the bandwidth of the kernel, which determines the spread of each paintball. Secondly, a saturation exponent which determines the hue of each paintball (the amount of information content). Both parameters were estimated using a cross-validation approach that partitioned the data into 80% training and 20% test, repeated 1,000 times. For each replicate, the training partition was used to generate interpolated maps (given a proposed bandwidth and saturation exponent) and a comparison was made at the locations of the test partition between the predicted values and the observed values. This comparison used a summary statistic that accounts for both the interpolated dairy residue frequencies and the confidence (saturation). A good answer (predicted frequency close to the observed frequency) is better than an uncertain prediction (low saturation) which is better than a bad answer, therefore we seek to maximize saturation for which predicted frequencies are accurate and minimize saturation for which predicted frequencies are poor. Therefore, our summary statistic was the magnitude of the difference between saturation and prediction accuracy, which was minimized when bandwidth = 6.18 and the saturation exponent = 0.0538 (Supplementary Fig. 9).

Reporting summary

Further information on research design is available in the Nature Research Reporting Summary linked to this paper.

Data availability

Data for running the aDNA analyses are available from https://github.com/ydiekmann/Evershed_Nature_2022. KML files, a summary of archaeological milk residue data, ecological proxy variables and a summary of radiocarbon dates are available from https://github.com/AdrianTimpson/2020-03-03523A. UK Biobank data are available from: https://www.ukbiobank.ac.uk/.

Code availability

R code for running the aDNA analyses is available from https://github.com/ydiekmann/Evershed_Nature_2022. Open-source R Code for running the UK Biobank analyses under MIT license are available from https://github.com/MRCIEU/lp-coevolution. R code for the generation of Figs. 1, 2, 3 and Extended Data Fig. 1 are available from https://github.com/AdrianTimpson/2020-03-03523A.

Extended Data Fig. 1 | Regional fluctuations in milk use throughout European prehistory. Percentage of milk fats through time, calculated using all animal fat residues. Grey bars and black lines illustrate 95%, 50% CI and MAP in each time slice, using a uniform prior.
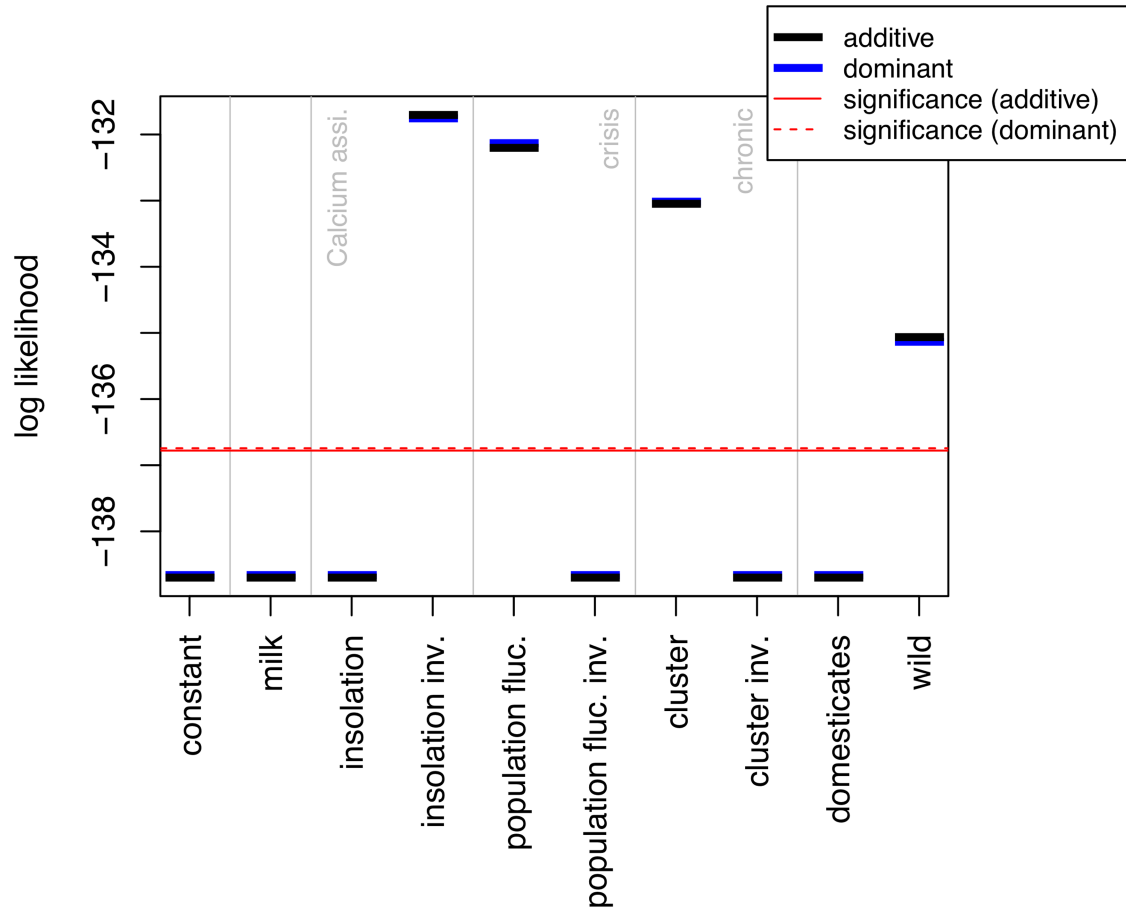
Extended Data Fig. 2 | Summary of model selection results for the tested ecological time series. Inverse solar insolation, fluctuations in population level, and residential density yield models significantly better than a null model of constant selection (significance computed by likelihood ratio test). See Extended Data Table 1 for corresponding parameter estimates, and multiple testing correction (no change in the set of significant models). *Abbreviations:* assimilation (assi.), inverse (inv.), fluctuation (fluc.).

Inverse insolation, additive (f_0 = 9e−04, **s** = 0.045, **a** = 0.503**)**
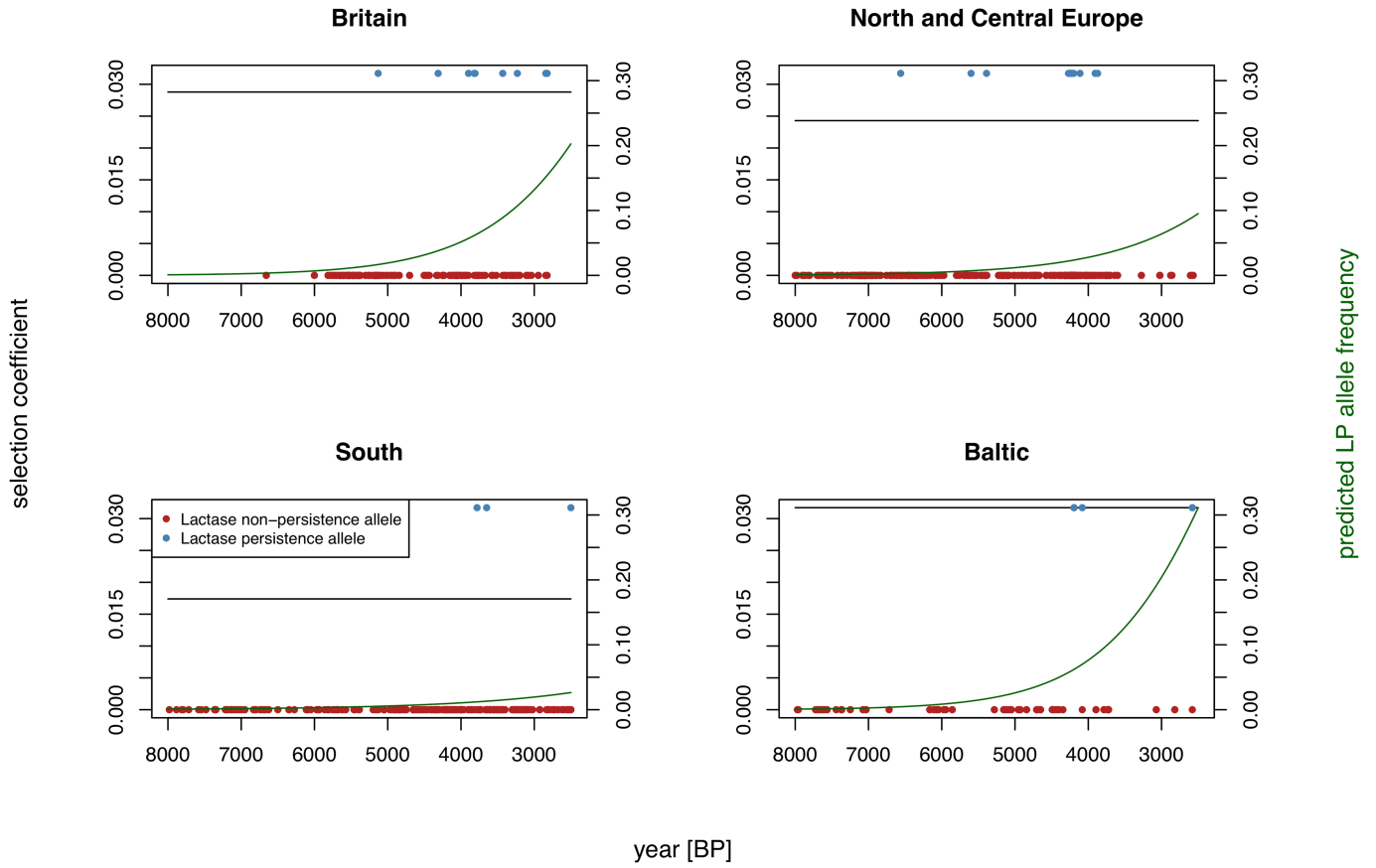
Extended Data Fig. 3 | Inverse insolation as a driver of selection strength. Optimized parameters, resulting selection strength- and LP allele frequency curves for inverse (inv.) insolation, one of the four ecological proxy variables yielding likelihoods significantly better than a constant selection model. Although LP is generally thought of as a dominant trait, we only show the additive model results as the parameter estimates barely differ.

Population fluctuation, additive (f_0 = 0.001, **s** = 0.147, **a** = 0.259**)**
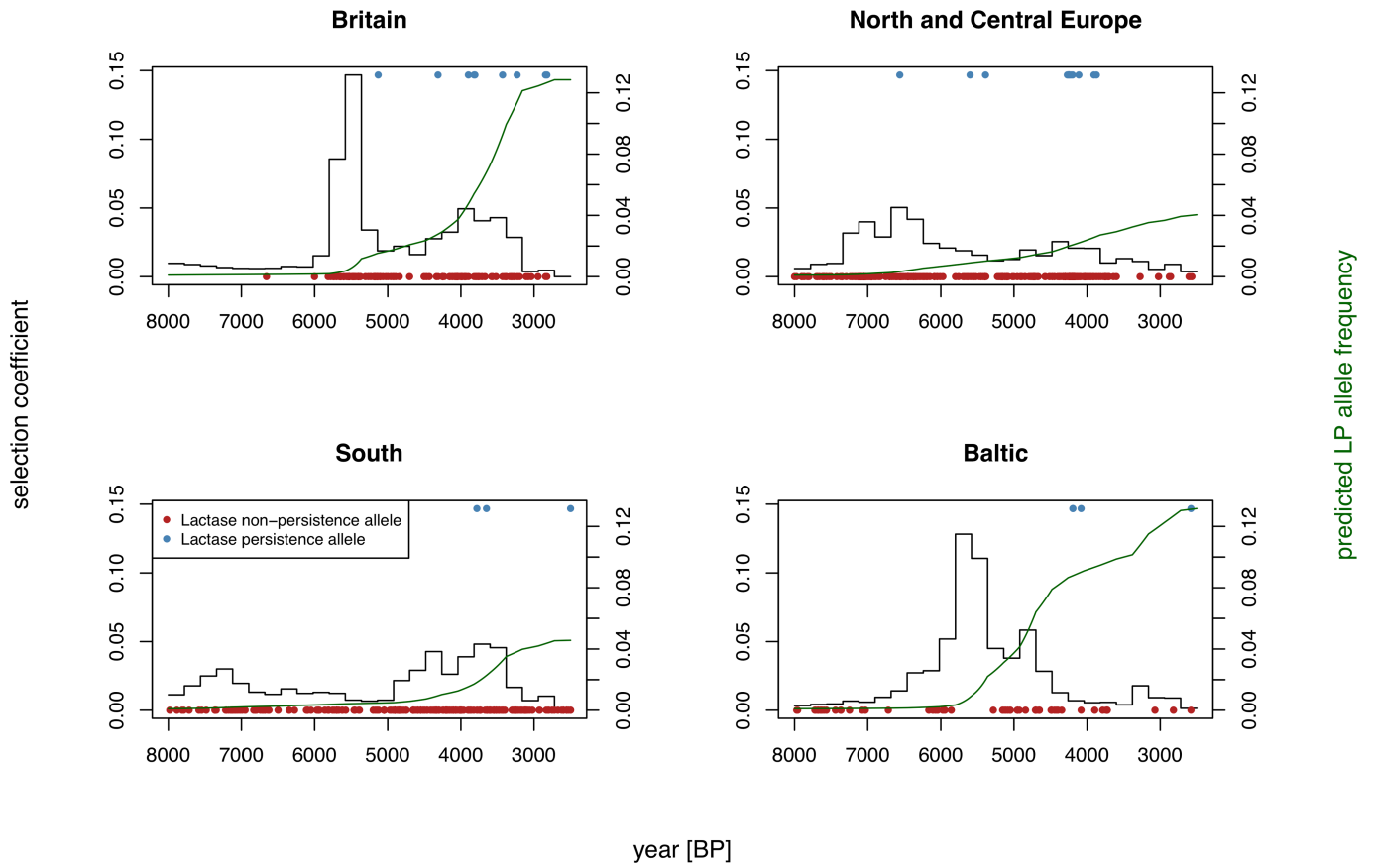
Extended Data Fig. 4 | Population fluctuation as a driver of selection strength. Optimized parameters, resulting selection strength- and LP allele frequency curves for population (pop.) fluctuations (fluc.), one of the four ecological proxy variables yielding likelihoods significantly better than a constant selection model. Although LP is generally thought of as a dominant trait, we only show the additive model results as the parameter estimates barely differ.

Settlement density, additive (f_0 = 7e−04, s = 0.036, a = 0.729)

Extended Data Fig. 5 | Settlement density as a driver of selection strength. Optimized parameters, resulting selection strength- and LP allele frequency curves for the cluster statistic, one of the four ecological proxy variables yielding likelihoods significantly better than a constant selection model. Although LP is generally thought of as a dominant trait, we only show the additive model results as the parameter estimates barely differ.
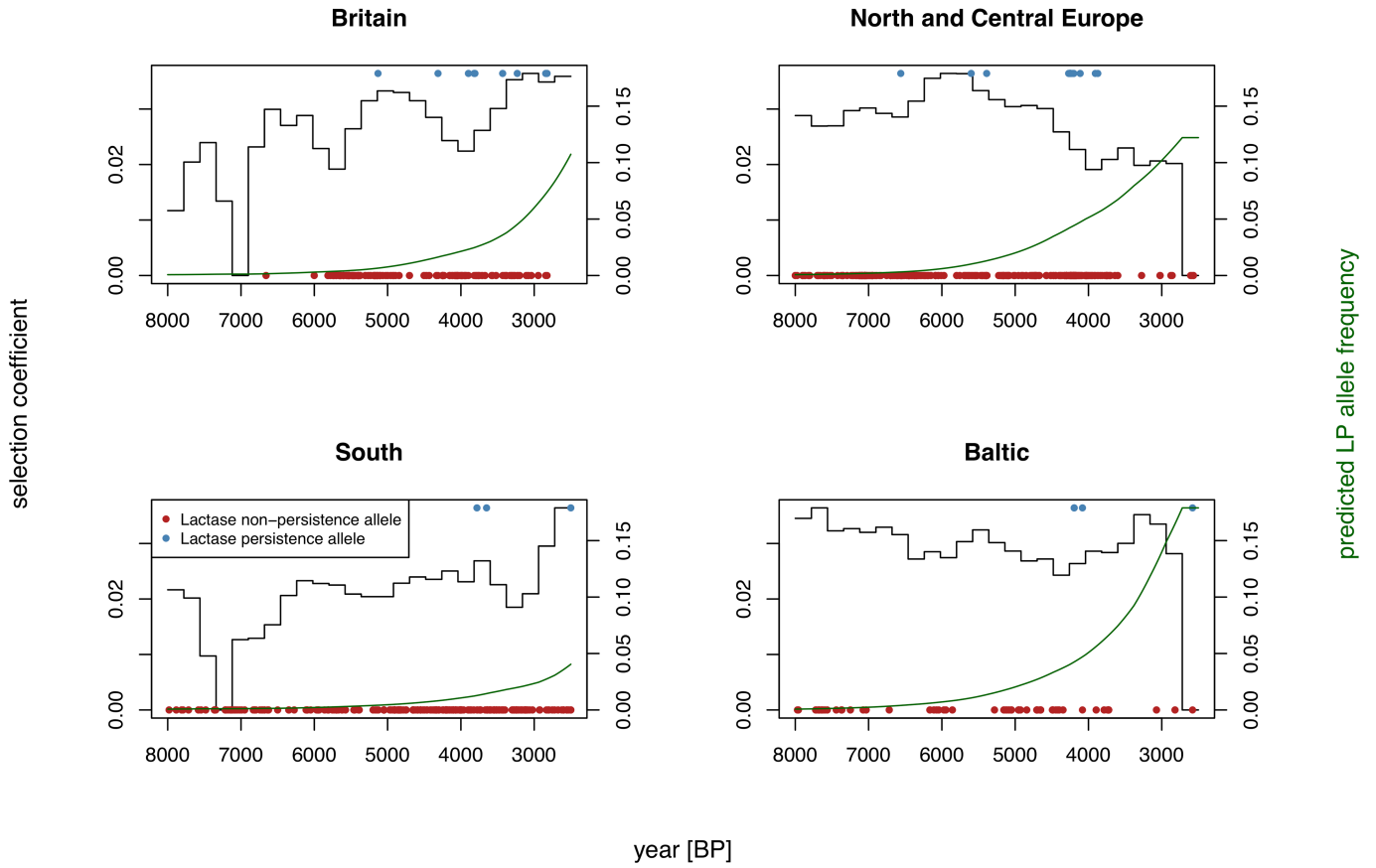
Extended Data Fig. 6 | Wild animal consumption as a driver of selection strength. Optimized parameters, resulting selection strength- and LP allele frequency curves for proportion of wild versus domestic animal, one of the four ecological proxy variables yielding likelihoods significantly better than a constant selection model. Although LP is generally thought of as a dominant trait, we only show the additive model results as the parameter estimates barely differ.
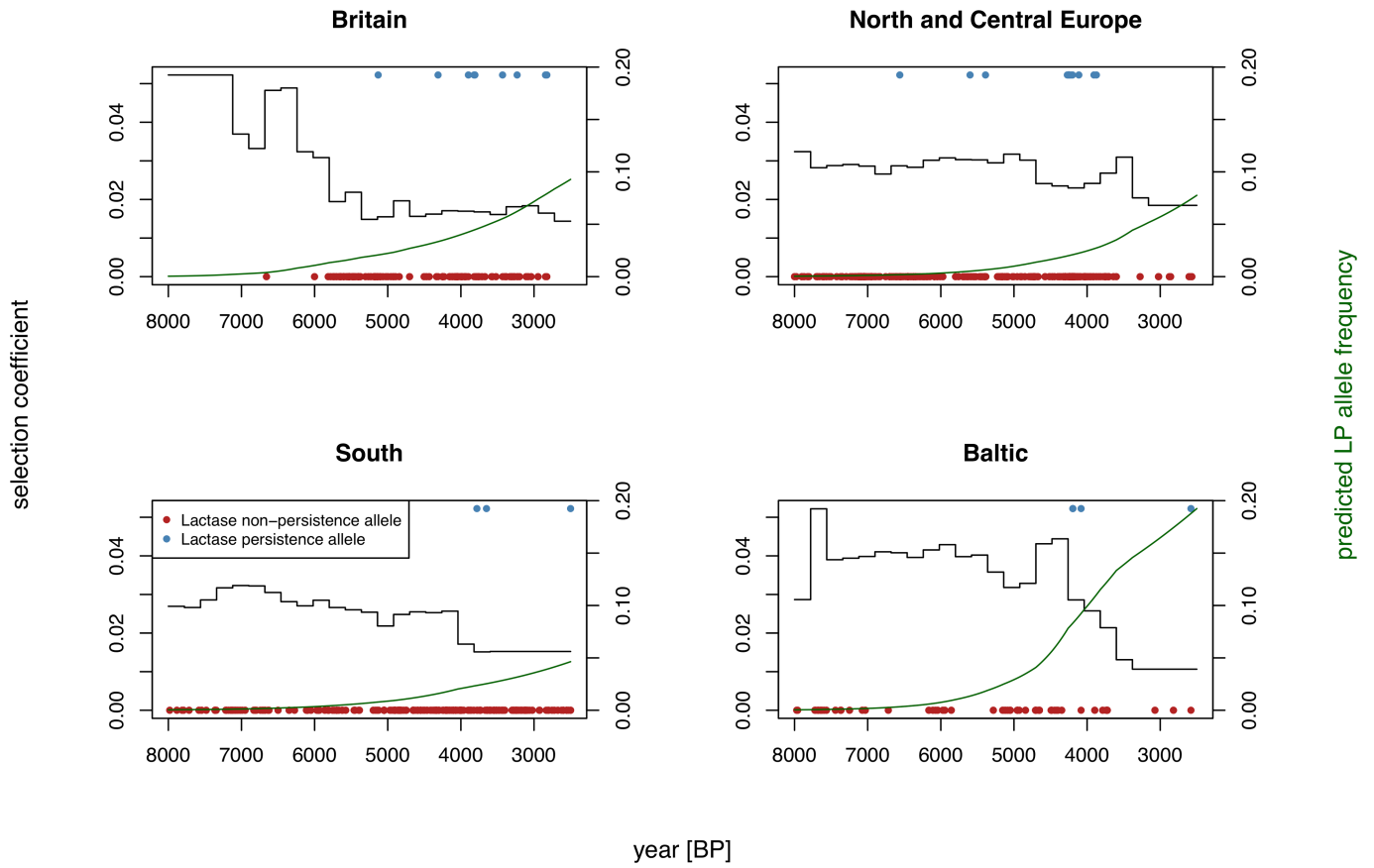
Extended Data Table 1 | Model selection results for the tested ecological time series

Model	nb. of par.	log. likelihood	LRT p-value	$\widehat{y_0}$	$\hat{s}$	$\hat{a}$	rank j; $\delta\frac{j}{9}$, $\delta = 0.02$	reject H_0?
constant, additive	2	-138.6995	*NA*	0.0013	0.022	*NA*	*NA*	*NA*
milk, additive	3	-138.6995	1	0.0013	0.022	1	8; 0.018	False
insolation, additive	3	-138.6995	1	0.0013	0.022	1	9; 0.02	False
insolation inv., additive	3	-131.7023	0.0002	9e−04	0.045	0.503	1; 0.002	True
population fluc., additive	3	-132.2044	0.0003	0.001	0.147	0.259	2; 0.004	True
population fluc. inv., additive	3	-138.6995	0.9997	0.0013	0.022	1	7; 0.016	False
cluster, additive	3	-133.0457	0.0008	7e−04	0.036	0.729	3; 0.007	True
cluster inv., additive	3	-138.6995	0.9997	0.0013	0.022	1	6; 0.013	False
domesticates, additive	3	-138.6995	0.9997	0.0013	0.022	1	5; 0.01	False
wild, additive	3	-135.0624	0.007	4e−04	0.052	0.696	4; 0.009	True
constant, dominant	2	-138.6642	*NA*	0.0012	0.011	*NA*	*NA*	*NA*
milk, dominant	3	-138.6642	0.9998	0.0012	0.011	1	8; 0.018	False
insolation, dominant	3	-138.6642	0.9997	0.0012	0.011	1	6; 0.013	False
insolation inv., dominant	3	-131.7533	0.0002	8e−04	0.024	0.496	1; 0.002	True
population fluc., dominant	3	-132.1293	0.0003	0.001	0.089	0.245	2; 0.004	True
population fluc. inv., dominant	3	-138.6642	0.9997	0.0012	0.011	1	5; 0.01	False
cluster, dominant	3	-133.0144	0.0008	7e−04	0.019	0.724	3; 0.007	True
cluster inv., dominant	3	-138.6642	0.9997	0.0012	0.011	1	7; 0.016	False
domesticates, dominant	3	-138.6642	0.9998	0.0012	0.011	1	9; 0.02	False
wild, dominant	3	-135.1375	0.0079	4e−04	0.028	0.687	4; 0.009	True

Columns 5–7 show the maximum likelihood parameter estimates. The last columns list the quantities needed for multiple testing correction by control of the false discovery rate via Benjamini–Hochberg procedure. The null hypothesis of constant selection is rejected at significance level δ, here $\delta = 0.02$, in favour of a fluctuating selection model when the p-value of the test with rank j is below $\delta\frac{j}{9}$, for which nine is the total number of hypothesis tests. Owing to the parametrisation of fitness, the dominant selection coefficient has to be multiplied by a factor 2 to be comparable to the additive models (see Methods section on ancient DNA analysis for details). *Abbreviations:* number (nb.), parameters (par.), logarithmic (log.), likelihood ratio test (LRT), inverse (inv.), fluctuation (fluc.).

Extended Data Table 2 | Lactase genotype frequency and test for departure from Hardy–Weinberg equilibrium

Population	AF	N	AA	GA	GG	P	x^2
			UK Biobank				
White, British	0.74	354926	197750	133022	24154	1.80×10^{-18}	76.93
White, Irish	0.84	10657	7528	2863	266	0.75	0.10
Any other white background	0.50	14732	4309	6117	4306	4.10×10^{-94}	423.57
White and Black Caribbean	0.51	203	44	121	38	5.90×10^{-3}	7.57
White and Black African	0.46	98	18	54	26	0.28	1.17
White and Asian	0.51	298	69	167	62	0.04	4.39
Any other mixed background	0.47	465	94	250	121	0.09	2.90
Indian	0.58	19	7	8	4	-	-
Pakistani	0.50	7	1	5	1	-	-
Any other Asian background	0.09	171	1	29	141	-	-
Caribbean	0.41	11	0	9	2	-	-
African	0.30	5	1	1	3	-	-
Any other Black background	0.75	4	2	2	0	-	-
Chinese	0.67	3	1	2	0	-	-
Other ethnic group	0.25	1561	199	384	978	2.90×10^{-42}	185.64
			gnomAD				
Amish	0.77	454	277	143	34	0.01	6.23
European (non-Finnish)	0.64	33992	14462	14270	5260	2.81×10^{-67}	300.32
European (Finnish)	0.58	5274	1754	2583	937	0.79	0.07
Other	0.29	1044	114	386	544	4.05×10^{-4}	12.51
Latino/Admixed American	0.23	7631	442	2593	4596	2.80×10^{-3}	8.93
South Asian	0.16	2412	92	603	1717	3.37×10^{-5}	17.19
Ashkenazi Jewish	0.13	1734	26	400	1308	0.46	0.54
African/African American	0.12	20694	328	4370	15996	0.14	2.21
Middle Eastern	0.07	158	3	15	140	-	-
East Asian	0.00	2599	1	9	2589	-	-

LP genotype (rs4988235-A) frequencies in UK Biobank (stratified by self-reported ethnic background, field 21000) and gnomAD v3 (accessed 11/07/2022) showing strong departure from Hardy–Weinberg equilibrium in European and East Asian populations. AF, allele frequency. N, sample size. AA, homozygous lactase persistent. GA, heterozygous lactase persistent. GG, homozygous LNP. P, chi-squared test for departure from Hardy–Weinberg equilibrium. X^2, chi-squared statistic.

Extended Data Table 3 | Lactase persistence genotype correlation between spousal pairs in UK Biobank

Test	N	Effect	95% CI		P
Additive	46,560	0.004	-0.002	0.011	0.22
Additive (sensitivity)	46,560	0.004	-0.003	0.010	0.26
Dominant	46,560	OR 1.10	1.001	1.220	0.05
Dominant (sensitivity)	46,560	OR 1.11	1.001	1.221	0.05

Association of individual lactase persistence genotype on spouse genotype adjusted for age, partner age, top ten genetic principal components and partner top ten genetic principal components. Sensitivity analyses were additionally adjusted for top 40 genetic principal components. Additive and dominant inheritance models were evaluated using linear and logistic regression, respectively. CI, confidence interval. N, sample size. OR, odds ratio.

Extended Data Table 4 | Proportion of significant likelihood differences between constant and fluctuating selection model driven by milk exploitation

		est. of $a < 0.95$			est. of $a \geq 0.95$		
N_e	initial freq.	all	nb. der. al. $\geq$ obs.	nb. der. al. $<$ obs.	all	nb. der. al. $\geq$ obs.	nb. der. al. $<$ obs.
NA	0.005	0.63	0.86	0.3	0.0	0.0	0.0
10,000	0.005	0.67	0.86	0.29	0.17	0.25	0.0
1,000	0.005	0.64	0.93	0.125	0.4	0.5	0.0

Proportions are given separately for models with parameter *a* close to one, as these are generally indistinguishable from constant selection models, and for simulations with less and at least the same number of derived alleles as observed in the real aDNA data. *Abbreviations:* frequency (freq.), estimate (est.), number (nb.), derived (der.), alleles (al.), observed (obs.).

Corresponding author(s):   Richard Evershed

Last updated by author(s):   Dec 3, 2021

Reporting Summary

Nature Research wishes to improve the reproducibility of the work that we publish. This form provides structure for consistency and transparency in reporting. For further information on Nature Research policies, see our Editorial Policies and the Editorial Policy Checklist.

Statistics

For all statistical analyses, confirm that the following items are present in the figure legend, table legend, main text, or Methods section.

n/a	Confirmed	
☐	☒	The exact sample size (*n*) for each experimental group/condition, given as a discrete number and unit of measurement
☐	☒	A statement on whether measurements were taken from distinct samples or whether the same sample was measured repeatedly
☐	☒	The statistical test(s) used AND whether they are one- or two-sided *Only common tests should be described solely by name; describe more complex techniques in the Methods section.*
☐	☒	A description of all covariates tested
☐	☒	A description of any assumptions or corrections, such as tests of normality and adjustment for multiple comparisons
☐	☒	A full description of the statistical parameters including central tendency (e.g. means) or other basic estimates (e.g. regression coefficient) AND variation (e.g. standard deviation) or associated estimates of uncertainty (e.g. confidence intervals)
☐	☒	For null hypothesis testing, the test statistic (e.g. *F*, *t*, *r*) with confidence intervals, effect sizes, degrees of freedom and *P* value noted *Give P values as exact values whenever suitable.*
☐	☒	For Bayesian analysis, information on the choice of priors and Markov chain Monte Carlo settings
☐	☒	For hierarchical and complex designs, identification of the appropriate level for tests and full reporting of outcomes
☐	☒	Estimates of effect sizes (e.g. Cohen's *d*, Pearson's *r*), indicating how they were calculated

Our web collection on statistics for biologists contains articles on many of the points above.

Software and code

Policy information about availability of computer code

Data collection	HP chemstation used for GC data acquisition. GC-MS control and acquisition used Xcalibur Thermo Scientific. Isotope Data acquisition was carried out using Ion Vantage software (version 1.5.6.0, IsoPrime) and Isodat 3.0.
Data analysis	HP chemstation used for GC data analysis GC-MS analysis used Xcalibur Thermo Scientific. Isotope data analysis was carried out using Ion Vantage software (version 1.5.6.0, IsoPrime) and Isodat 3.0. R code used for downstream data analysis available of public repositories.

For manuscripts utilizing custom algorithms or software that are central to the research but not yet described in published literature, software must be made available to editors and reviewers. We strongly encourage code deposition in a community repository (e.g. GitHub). See the Nature Research guidelines for submitting code & software for further information.

Data

Policy information about availability of data

All manuscripts must include a data availability statement. This statement should provide the following information, where applicable:
- Accession codes, unique identifiers, or web links for publicly available datasets
- A list of figures that have associated raw data
- A description of any restrictions on data availability

All data generated during this study are available on request or published in publicly accessible data bases. R Code for running the UK Biobank analyses are available from: https://github.com/MRCIEU/lp-coevolution. R and Python code for running the Ancient DNA analyses are available from: https://github.com/ydiekmann/Evershed_Nature_2022. R code for processing model variables , mapping and summary archaeological and isotopic data is available at https://github.com/AdrianTimpson/2020-03-03523A

Field-specific reporting

Please select the one below that is the best fit for your research. If you are not sure, read the appropriate sections before making your selection.

☐ Life sciences ☐ Behavioural & social sciences ☒ Ecological, evolutionary & environmental sciences

For a reference copy of the document with all sections, see nature.com/documents/nr-reporting-summary-flat.pdf

Ecological, evolutionary & environmental sciences study design

All studies must disclose on these points even when the disclosure is negative.

Study description	Analysis of human genetic selection using a large scale collation and analysis of novel and existing archaeological and modern data comprising organic residue composition and isotope values, demographic proxy data comprising radiocarbon and faunal remains, and ancient human DNA.
Research sample	UK Biobank cohort study of approximately 500,000 UK participants aged 37-73 years , containing wide-range of measures including demographics, health status, lifestyle, cognitive function, mental and physical health and molecular data such as genetic and biomarkers. BAM files from 674 ancient Eurasian individuals aligned to the GRCh37/hg19 human reference assembly. Demographic proxy data constructed using >110,000 radiocarbon dates compiled from over 1,000 published sources. Organic residue data for 6,610 animal fat residues derived from >12,700 potsherds from 527 archaeological sites.
Sampling strategy	Our objective was to include all available data across Europe.
Data collection	Novel and existing data was collated from published literature and databases, and where appropriate was aggregated into a MySQL Relational database
Timing and spatial scale	The study focuses on Europe. Archaeological data spans c.7kyrBCE to 1kyrCE, and ancient human DNA also extends into Asia.
Data exclusions	Beyond standard quality control, we took a fully inclusive approach to all relevant data.
Reproducibility	Results and analysis are fully reproducible using our publicly available methods and data.
Randomization	Randomization was not required, since we utilized all published and novel data to maximize sample sizes.
Blinding	Novel organic residue data acquisition was achieved through a largely automated pipeline. Any potential human influence from lab technicians remains blind to the archaeological contexts of samples.

Did the study involve field work? ☐ Yes ☒ No

Reporting for specific materials, systems and methods

We require information from authors about some types of materials, experimental systems and methods used in many studies. Here, indicate whether each material, system or method listed is relevant to your study. If you are not sure if a list item applies to your research, read the appropriate section before selecting a response.

Materials & experimental systems

n/a	Involved in the study
☒	Antibodies
☒	Eukaryotic cell lines
☒	Palaeontology and archaeology
☒	Animals and other organisms
☒	Human research participants
☒	Clinical data
☒	Dual use research of concern

Methods

n/a	Involved in the study
☒	ChIP-seq
☒	Flow cytometry
☒	MRI-based neuroimaging